Evaluating the Performance of Denitrifying Bioreactors for Removal of Agricultural Nitrate from Tile-Drainage Effluent

Corey Flemming

A thesis submitted to the
Faculty of Graduate and Postdoctoral Studies
in partial fulfillment of the requirements for the
MSc degree in Earth Sciences (Env. Sus.)

Department of Earth and Environmental Sciences
Faculty of Science
University of Ottawa

Table of Contents

List of Tables

List of Figures

Abstract

The application of nitrogen (N) fertilizers and manure to agricultural soil is essential for crop production, but has in turn introduced environmental impacts including: eutrophication, contamination of groundwater, freshwater acidification, and an increase in greenhouse gas emissions. The movement of nitrogen was observed following liquid swine manure applications at six fields in Winchester, ON employing controlled tile drainage and denitrifying bioreactors. The manure was mainly in the form of ammonium during application where it was transformed to other N species including nitrate and nitrous oxide (N_2O) by microbial activity in soil. Large soil N_2O fluxes occurred in fields throughout 2012 and 2013, and total N of soil in the fields was enriched in ^{15}N, indicating denitrification. Soil nitrate was also leached and collected by drainage tiles, and a portion of the tile water was treated by denitrifying bioreactors. Previous studies have demonstrated that denitrification of nitrate in bioreactors elicits the production of N_2O, which is emitted from the overlying soil surface and/or is released as dissolved N_2O in tile effluent. In this study, it is found that a decrease in nitrate was associated with decreasing levels of nitrous oxide during a rain event, and no significant N_2O flux was recorded above bioreactors throughout either year. The $\delta^{15}N$ and $\delta^{18}O$ signatures of nitrate did not change significantly following bioreactor treatment and did not exhibit the ^{15}N and ^{18}O enrichment that is characteristic of denitrification. The data demonstrates that the decrease in nitrate through the bioreactors was due to dilution, likely from the accumulation of rainfall in reactor beds employing controlled tile drainage. Further work is needed to examine the conditions under which dilution may occur in place of denitrification.

Abstrait

L'application des engrais azotes (N) et du fumier dans le sol agricole est essentielle pour la production de récolte, mais a à son tour introduit des impacts environnementaux y compris : l'eutrophisation, la contamination des eaux souterraines, l'acidification d'eaux douces et une augmentation des émissions de gaz à effet de serre. Le mouvement de l'azote a été observé suite aux applications de fumier de porc dans six champs à Winchester, ON en utilisant le drainage controlé par canalisations enterrées la dénitrification de bioréacteurs. Le fumier était sous la forme d'ammonium lors de l'application où il a été transformé à d'autres espèces N, y compris le nitrate et l'oxyde nitreux (N_2O) par l'activité microbienne dans le sol. De grands flux N_2O ont eu lieu dans le sol tout au long de 2012 et 2013 et le total N du sol dans les champs a été enrichis en ^{15}N indiquant la dénitrification. Le nitrate du sol a également été lessivé et recueillis par le drainage controlé par canalisations enterrées et une portion de l'eau de tuyaux a été traitée par dénitrification bioréacteurs. Des études antérieures ont démontré que la dénitrification de nitrate dans des bioréacteurs provoque la production de N_2O, qui est émise à partir de la surface du sol sus-jacente et/ou relâcher à l'état dissous N_2O de l'effluent de tuyaux. Dans cet etude, il est constate qu'une diminution des nitrates était associée à une diminution des niveaux d'oxydes d'azote lors d'un événement pluvieux, et aucun flux significatif de N2O a été enregistrée au-dessus de bioréacteurs tout au long de chaque année. Les signatures $\delta^{15}N$ et $\delta^{18}O$ de nitrate n'a pas changé de manière significative après le traitement de bioréacteur et ne présentent pas l'enrichissement ^{15}N and ^{18}O qui est caractéristique de la dénitrification. Les données démontrent que la diminution de nitrate à travers les bioréacteurs était due à la dilution, probablement de toute l'accumulation de précipitations dans des lits de réacteur utilisant le drainage controlé par

canalisations enterrées. Des travaux supplémentaires sont nécessaires pour examiner les conditions dans lesquelles la dilution peut se produire à la place de dénitrification.

Acknowledgements

I would first like to express my gratitude to my thesis advisor Dr. Ian Clark of the University of Ottawa. The door to Dr. Clark's office was always open for discussion and guidance. Thank you to Dr. Alisha Van Zandvoort, I couldn't have asked for a better partner on this project, and through years of fieldwork and labwork. Thank you to Dr. David Lapen for guidance and support in executing this project.

I would also like to thank the following experts from Agriculture and Agri-Food Canada and the University of Ottawa, who were involved with various stages of fieldwork, lab analysis, data analysis, and overall guidance: Emilia Craiovan, Mark Edwards, Shan Shan Wu, Natalie Gottschall, Paul Middlestead, Wendy Abdi and Patricia Wickham. Without their participation and input, such an intensive fieldwork and lab analysis program would not have been possible.

Finally, I must express my very profound gratitude to my parents and to my fiancée Jamie-Lynn for providing me with support and continuous encouragement throughout my years of study and through the process of researching and writing this thesis. This accomplishment would not have been possible without you. Thank you!

1. Introduction

Nitrogen availability in agriculture is a key limitation to biomass production, and was resolved by the invention of the Haber-Bosch process of industrial N fixation in the early 20th century (Smil, 2002b). The rate of nitrogen fixation by the Haber-Bosch process surpassed natural N fixation in the 1970s (Galloway et al., 2003) and continues to climb. Modern agriculture is now reliant on synthetic fertilizer inputs which feed approximately 50% of the world's population (Erisman et al., 2008). Nitrogen can also be applied to agricultural soils as manure, where N excreted by livestock is essentially recycled. The addition of N to soils, whether by fertilizer or manure, has come at the cost of multiple environmental impacts including: coastal eutrophication (Duarte, 2009), freshwater acidification (Lepori and Keck, 2012), contamination of groundwater and contributions to the greenhouse effect (IPCC, 2007a).

In 1998, Galloway (1998) coined the term Reactive N (N_r), which encompasses all forms of N other than N_2 gas. By grouping N_r, a budget for N can be simplified to consider only the fixation of N_2 to a reactive form, and its eventual transformation back to N_2 gas via denitrification or anammox. The amount of reactive N continues to increase globally due to industrial N fixation, NO_x emissions from combustion, and an increase in nitrogen fixing legume crops (Fields, 2004; Galloway et al., 2003).

The global nitrogen cycle is now strongly influenced by anthropogenic processes, a major shift from a century ago. Crop and livestock production produces a large anthropogenic impact on global N cycle (Bouwman et al., 2013). A primary research goal in agriculture is to increase the efficiency of nitrogen uptake by humans while reducing N loss to the environment. In order to address this, we must first understand the fate of anthropogenic N_r and identify potential key

areas of improvement. Humans ultimately consume only a fraction of soil N fertilizer input, and the remainder is lost to the environment. In food crop production, approximately 70% of N is made available for human consumption, while in livestock production, only about 15% of N from feed crops is made available (Smil, 2002a). One possible means of increasing N uptake efficiency is therefore to decrease meat consumption in human diet, while other measures involve optimizing crop and livestock production systems to increase N uptake by crops and livestock, minimize loss to the environment, and to convert unused N_r to N_2. As the amount of N_r continues to increase, international action is required to increase N use efficiency (Fowler et al., 2015).

1.1 Fertilization of Agricultural Fields

In order to sustain annual crop production, agricultural soils require the replenishment of vital nutrients and organic matter. Nitrogen is typically the most limiting nutrient and corn plants in particular require significant nitrogen inputs for proper growth (Millar et al., 2010). Synthetic fertilizers and/or manure may be used to replenish soil nitrogen; however, manure applications have the benefit of including a host of other nutrients and minerals, and organic matter, which can improve drainage, water retention and stimulate the microbial community (De Freitas et al., 2003; Zingore et al., 2007). Liquid swine manure is commonly used as a fertilizer for corn crops since a large fraction of its N content is available immediately to plants as ammonium-N, and nitrogen can be applied in sufficient quantity without over applying other nutrients such as Potassium (K) or Phosphorus (P).

In Canada, manure is typically applied in either the spring or fall, and there are trade-offs to both approaches. For spring manure applications, it is ideal to time the application as close as possible

to the date of planting. This helps maximize the uptake of available nutrients by plants and reduces the amount of N available for leaching. Spring application can be inconvenient in practice however, since it leaves a small window to time application, tillage and planting; especially in humid regions where soil moisture may limit field trafficability. Fall application may produce less N_2O emissions (Hernandez-Ramirez et al., 2009), and allows more time for mineralization of the organic component of the manure to plant-available forms of N. If applied in relatively dry regions with fine textured soils, this may allow a greater amount of plant-available N to be present from the same quantity of manure. On the other hand, in relatively wet regions or regions with coarser textured soils, there is a high risk of leaching resulting in less available N for plants during the growing season. Significant volatilization of ammonium-N from fall-applied manure can also occur if left on the surface, and can be reduced by soil tillage or sub-surface injection (Huijsmans, 2003).

1.2 Common Nitrogen-Related Reactions in Soil

Nitrogen in manure is present mainly as organic N and ammonium-N (Beauchamp, 1986). A variety of reactions can occur in agricultural soils, resulting in the conversion of N to other forms (Butterbach-Bahl et al., 2013). Mineralization of organic N in manure can occur as a by-product of the decomposition of organic matter. The result is the conversion of organically-bonded N to ammonia (NH_3), which then reacts with water to form ammonium (NH_4^+), a plant-available form of N. Under aerobic conditions, nitrification may proceed where autotrophic bacteria in soil oxidize NH_4^+ to nitrite (NO_2^-) and then to nitrate (NO_3^-), also a plant-available form of N, as shown in the following equations taken from EPA (2002).

Oxidation of Ammonium to Nitrite by *Nitrosomonas*:

$$NH_3 + O_2 \rightarrow NO_2^- + 3\ H^+ + 2\ e^-$$

Oxidation of Nitrite to Nitrate by *Nitrobacter*:

$$NO_2^- + H_2O \rightarrow NO_3^- + 2\ H^+ + 2\ e^-$$

In anaerobic or oxygen-poor soils, NO_3^- may be converted to N_2 via denitrification or anaerobic ammonium oxidation (anammox). In the case of denitrification, nitrate is reduced through several intermediate forms, including $N_2O_{(g)}$, to $N_{2\,(g)}$ (Bernhard, 2010).

Incremental reduction of N during denitrification:

$$NO_3^- \rightarrow NO_2^- \rightarrow NO + N_2O \rightarrow N_2$$

Net redox reaction for the denitrification of nitrate:

$$2\ NO_3^- + 10\ e^- + 12\ H^+ \rightarrow N_2 + 6\ H_2O$$

An anammox reaction oxidizes ammonia and reduces nitrite to form dinitrogen gas directly (Bernhard, 2010), and does not produce the greenhouse gas N_2O:

Anaerobic ammonium oxidation (anammox) reaction:

$$NH_4^+ + NO_2^- \rightarrow N_2 + 2\ H_2O$$

1.3 Canadian Agricultural Greenhouse Gas Emissions

In Canada, greenhouse gas (GHG) emissions from agriculture account for approximately 8% of total national GHG emissions, excluding land-use and land-use change (Environment Canada, 2013). The main GHGs emitted in Canadian agriculture are methane (CH_4), occurring primarily from enteric fermentation during cattle production, and nitrous oxide (N_2O) from N fertilizer and

manure application to agricultural soils (Environment Canada, 2015b). Canada's agricultural GHG emissions remained relatively stable from 2005 to 2013; however, increasing emissions from crop production and on-farm fuel use are currently being offset by a reduction in emissions from livestock (Environment Canada, 2015b). Agricultural soils provide a significant contribution to Canada's emissions trend, mainly via nitrous oxide (N_2O) emissions. N_2O is a powerful greenhouse gas with a global warming potential 298 times that of CO_2 for a 100-yr time horizon (IPCC, 2007b). Nitrogen fertilizer sales have more than doubled since 1990 and continue to rise (Environment Canada, 2015b; Statistics Canada, 2015). Soil GHG emissions can be broken down into direct emissions, which originate from the production site, or indirect emissions, which are the result of leached and volatilized N being emitted outside of the agricultural production site. In addition to indirect GHG emissions, the fraction of N that is leached from agricultural soils has the potential to contaminate the surrounding environment. These impacts can be managed with modern drainage management practices, by reducing the export of N in tile drainage and facilitating the transformation of reactive N back to N_2.

1.4 Agricultural Best Management Practices

Agricultural Best-Management Practices (BMP's) are farming methods outlined in a series of publications, that aim to reduce the environmental impact of farming while maintaining economic productivity (Agriculture and Agri-Food Canada, 2000; OMAFRA, 2016). One group of BMPs focuses on cropland drainage, and the proper implementation of subsurface drainage.

1.4.1 Controlled Tile Drainage

Tile drainage is an artificial drainage practice with growing popularity in humid regions where elevated water tables can impede crop production, particularly in spring. Cropland drainage is improved by installing a series of perforated tiles below the soil surface, which capture and relocate soil water to drainage ditches. Direct effects of this practice are an extended growing season and improved moisture conditions for crop growth, allowing for increased agricultural intensification and productivity (Fraser, 2001). Conversely, subsurface drainage can also act as an efficient means of agricultural N transport to surface water (Lapen et al., 2008). In addition to the negative environmental implications, nitrogen leaching and runoff represents a financial disincentive for farmers who wish to maximize fertilizer use efficiency.

Controlled tile drainage (CTD) is an alternative to free tile drainage which allows farmers to manage water table height during the growing season by restricting tile flow below a specified level. Whereas with free tile drainage, any water collected by the tile system is free to flow out of the field unobstructed, a controlled tile drainage system places a height-adjustable stop-gate between the drainage tiles and the drainage ditch. Water must flow over the stop-gate in order to exit the field. A minimum level of water is therefore held within the field, which is beneficial especially during dry summer months. Benefits of CTD include an increase nutrient uptake by plants (Sunohara et al., 2014), optimized soil moisture during dry months, reduced nutrient loss and increased crop yields (Crabbé et al., 2012; Rozemeijer et al., 2016).

1.4.2 Denitrifying Bioreactors

Denitrifying bioreactors are another recent agricultural management practice intended to reduce nutrient loading in agricultural runoff by facilitating the denitrification of NO_3^- to N_2, and

therefore removing reactive N from the environment. In a field employing a denitrifying bioreactor system, nutrient-rich tile water is passed through a reactor bed filled with carbon-rich media prior to exiting the field. This serves to increase the availability of carbon as an electron donor for denitrification, and can be optionally mixed with alum to simultaneously remove phosphorus. Woodchips are commonly used as the source of carbon; however, other sources such as rice straw, wheat straw, cotton, and maize cobs have been tested with varying degrees of success (Liang et al., 2015; Warneke et al., 2011c). Moorman et al. (2010) found that the population of denitrifying bacteria in bioreactor woodchips was as much as two orders of magnitude greater than in adjacent soils.

A considerable reduction in downstream nitrate loading is possible in agricultural areas with elevated N (Bock et al., 2015; Liang et al., 2015), and Christianson et al. (2011b) found higher N removal efficiency as inflow concentration decreased. Nitrate-N removal rates are limited primarily by carbon availability, temperature and retention time (Christianson et al., 2011a; Warneke et al., 2011c). Nitrogen removal efficiency of bioreactors have been shown to improve when combined with controlled tile drainage due to an increase in residence time (Woli et al., 2010).

During the denitrification of NO_3^-, a portion of N is released as N_2O adding to agricultural GHG emissions, and this fraction varies with oxygen availability (Khalil et al., 2004). A decrease in dissolved nitrate alone following bioreactor treatment is not sufficient evidence of denitrification since the same effect can occur from anaerobic ammonium oxidation (anammox) or dilution. It is therefore necessary to investigate the N removal performance of bioreactors to determine how and when N is leaving the field, in order to confirm proper functioning and maximize the efficiency of the system. The simultaneous behaviour of other dissolved N species can be

examined, such as ammonium or N_2O, in order to pinpoint the underlying processes. Stable isotope analysis of $^{15}N/^{14}N$ is one such tool for identifying transformation of N between pools and can be used to confirm the presence of denitrification.

1.5 Use of N Isotopes to Trace the Nitrogen Cycle

Nitrogen has two stable isotopes, ^{14}N and ^{15}N which are present in nature with natural abundances of approximately 99.6% and 0.4%, respectively. The ratio of ^{15}N:^{14}N in a given sample can be measured using a mass spectrometer and compared against that of ambient air to give $\delta^{15}N$ in permil. Ambient air is used as the standard for reporting $\delta^{15}N$ values.

$$\delta^{15}N = \left[\frac{\left[\frac{^{15}N}{^{14}N}\right]_{sample}}{\left[\frac{^{15}N}{^{14}N}\right]_{air}} - 1\right] \times 1000 \qquad \textbf{Equation 1}$$

The isotopic signature of each N species is equal to its parent species plus any fractionation that occurred during transformation. There are several types of fractionation. Those driven by biological processes are typically kinetic isotope reactions, where there is a unidirectional process favouring one stable isotope. Kinetic fractionation can also occur as diffusion of a gas through a porous medium or air column, where the mass difference between isotope species affects their relative velocities and leaving the substrate with a greater proportion of the heavier isotope. Kinetic isotope fractionation almost always results in the depletion of the end product and enrichment of the substrate (Shearer, 1989). This occurs as a Rayleigh distillation – the exponential enrichment of a finite reactant as it is converted to the end product:

$$R = R_0 f^{(\alpha-1)} \qquad \textbf{Equation 2}$$

Where:

R = Isotope ratio of the reservoir

R_0 = Initial isotope ratio of the reservoir

f = Remaining fraction of the reservoir

α = fractionation factor for the reaction

This relationship can also be expressed in δ-‰ notation and graphed to illustrate a Rayleigh distillation (Clark, 1997):

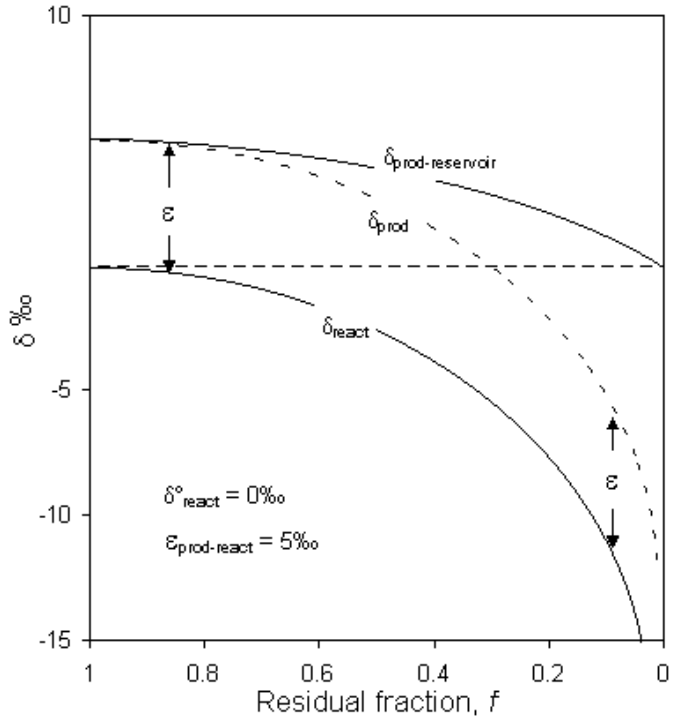

Figure 1: Rayleigh distillation of a reactant reservoir. *Adapted from "Environmental Isotopes in Hydrogeology" by Ian Clark and Peter Fritz, 1997, Ch.2, p.56. Copyright 2015 by CRC Press, LLC.*

In an open system, the product is immediately removed as it is formed and does not mix as a product reservoir (dashed line). In a closed system, the product accumulates and mixes, therefore its isotopic signature represents the sum of the product at a given fraction. The isotope ratio of a complete Rayleigh distillation (f=0) in a closed system is equal to that of the original reactant, conserving the mass balance of the system. This may occur in an extremely efficient closed system, for example during commercial N-fixation via the Haber-Bosch process where nearly 100% of atmospheric N_2 is reacted to NH_3 (Michalski et al., 2015). Otherwise, the isotope ratio of the product will deviate from the initial reactant, depending on the enrichment factor and the residual fraction remaining.

In agriculture, kinetic fractionation occurs during several different N transformations. Mineralization of N occurs where organic N is decomposed to ammonia (NH_3^+) and ultimately to ammonium (NH_4^+). The associated fractionation results in ^{15}N-depleted ammonia and ^{15}N enriched manure organic N. Manure also contains a significant amount of ammonia from urine. Ammonia is readily volatilized, favouring the lighter ^{14}N component via diffusive fractionation, and leaving the remaining ammonia relatively enriched in ^{15}N. Further isotope effects occur during oxidation of ammonium to nitrite (NO_2^-) by *Nitrosomonas* (Delwiche and Steyn, 1970) with an associated isotope effect between +14‰ and +38‰ (Casciotti et al., 2003; Mariotti et al., 1981; Yoshida, 1988) and during oxidation of nitrite to nitrate (NO_3^-) by *Nitrobacter* (Burns et al., 1995; Casciotti, 2009) with an isotope effect of -12.8‰ (Casciotti, 2009). The resulting nitrate is therefore expected to be depleted in ^{15}N compared with its parent species.

Complete denitrification occurs via microbial transformation of NO_3^- to $N_{2(g)}$ through a series of intermediate reactions. Nitrate is reduced from NO_3^- to NO_2^- with an associated ^{15}N enrichment between +13‰ and +30‰ (Barford et al., 1999; Delwiche and Steyn, 1970; Granger et al.,

2006), from NO_2^- to NO with an ^{15}N enrichment factor between +5‰ to +25‰ (Casciotti, 2009), from NO to N_2O (enrichment factor not available) and from N_2O to N_2 with an ^{15}N enrichment factor between +4‰ and +13‰ (Barford et al., 1999; Ostrom et al., 2007). The mean overall isotope effect of residual nitrate from denitrification of NO_3^- to N_2 has been estimated at between +20‰ and +30‰ for ^{15}N and +10‰ to +15‰ for ^{18}O (Kendall and Aravena, 2000; Létolle, 1980).

1.5.1 Identification of Dilution

Stable isotope analysis can be used to identify denitrification and clearly distinguish it from dilution. Whereas both processes will reduce nitrate concentration, denitrification has an associated ^{15}N-NO_3 enrichment factor of at least +20‰, and will simultaneously enrich residual nitrate according to a Rayleigh distillation. In the case of dilution, ^{15}N-NO_3 remains the same with minor fluctuations possible due to natural variability. The distinction is illustrated in Clark (2015):

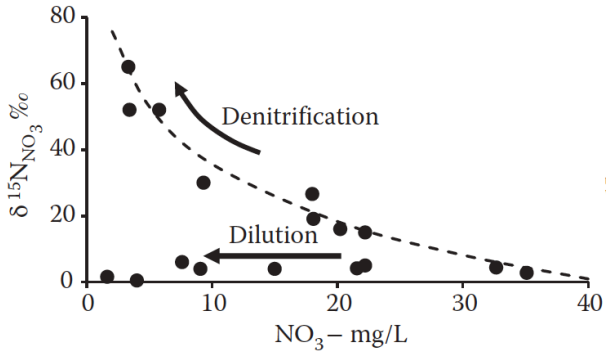

Figure 2: Behaviour of ^{15}N during nitrate attenuation by reaction and by dilution. *From "Groundwater Geochemistry and Isotopes" by Ian Clark, 2015, Ch.9, p.317. Copyright 2015 by Taylor and Francis Group, LLC.*

1.6 Research Description

This research aimed to explore the movement of agricultural N from application to groundwater, through a controlled tile drainage system and a denitrifying bioreactor, and to evaluate the performance of denitrifying bioreactors. Precipitation events over nutrient rich manure applications have the potential to load drainage tiles with highly concentrated leachate, and move the tile water rapidly through the bioreactor systems. The hypothesis was that a portion of N from applied manure would be emitted from soil as N_2O while another portion would leach and be captured by the drainage system. Also, we hypothesized that denitrification of nitrate would occur within the reactor beds, releasing a fraction of nitrate-N as N_2O, and enriching $\delta^{15}N$ and $\delta^{18}O$ of nitrate due to the kinetic fractionation associated with denitrification.

2. Site Description

This study area is a parcel of agricultural land located in Winchester, Ontario, Canada, approximately 60 km south of Ottawa and ~20 km north of the U.S. border (45.0618, -75.3423). This region lies within the watershed of the South Nation River, which flows northeast from Brockville, ON into the Ottawa river just north of Plantagenet, ON. The site topography is level to slightly undulating, and as a result of the relatively flat topography, surface runoff is minimal. The principal soils are a dark grey Gleisolic silt loam from the Osgoode series. The soils are a medium textured lacustrine deposit with poor drainage and consist of 6 inches of very dark grey loam and silt loam underlain by olive grey silt loam underlain by highly mottled silt loam and loam (Matthews, 1952). The 30-yr mean precipitation for the area is 84.8 mm in May, and 954.3 mm annually. The 30-yr mean minimum/maximum daily air temperature in May is 6.8°C/18.4°C (Environment Canada, 2015a).

The land was divided into two groups of three fields, each measuring ~15 m wide with a total area of approximately 0.15 Ha. Each of the six fields contains a controlled tile drainage system feeding into a woodchip bioreactor. Piezometer wells were installed at 90 cm, 120 cm and 200 cm depths below surface, at the front and back of each field in order to sample groundwater. A weather station was present on site recording air temperature, local air pressure, and humidity. When local climate data was unavailable, data from the nearest Environment Canada climate station (Kemptville) was used.

The controlled tile drainage system, in each field, consisted of multiple tile laterals joined downstream by a header tile directing water to a control structure. The drainage tiles were located approximately 1 m below soil surface with a slight slope towards the header tile at the

front of the fields. Water flowing through the control structure can either enter the bioreactor, or bypass the bioreactor depending on the flow rate and relative gate height of the bypass control structure.

Figure 3: Satellite image of the Winchester site showing the location of fields T1-T6

2.1.1 Bioreactors

Bioreactors were installed on all six drainage tiles in October of 2011 and designed to treat 20% of a peak flow of 2 L s^{-1}. The base and walls of each bed were lined with 12 mil plastic, filled with substrate and covered with a geotextile fabric (MarFil 20). Bioreactors contain one of three different amounts of aluminum sulfate (alum) mixed with hardwood woodchips in order to evaluate the removal of phosphorus as part of a separate study. The woodchips were ~5 cm^2 in surface area and 5.0 cm^3 in volume and were sourced from Greely Sand & Gravel Inc. Each reactor measured 2.4 m x 1.5 m x 0.9 m, for a total volume of approximately 3.2 m^3, and was overlain by ~0.5 m of topsoil. The woodchip-alum mixtures are given in **Table 1**, but were not considered in this work because there was no expected impact to nitrogen.

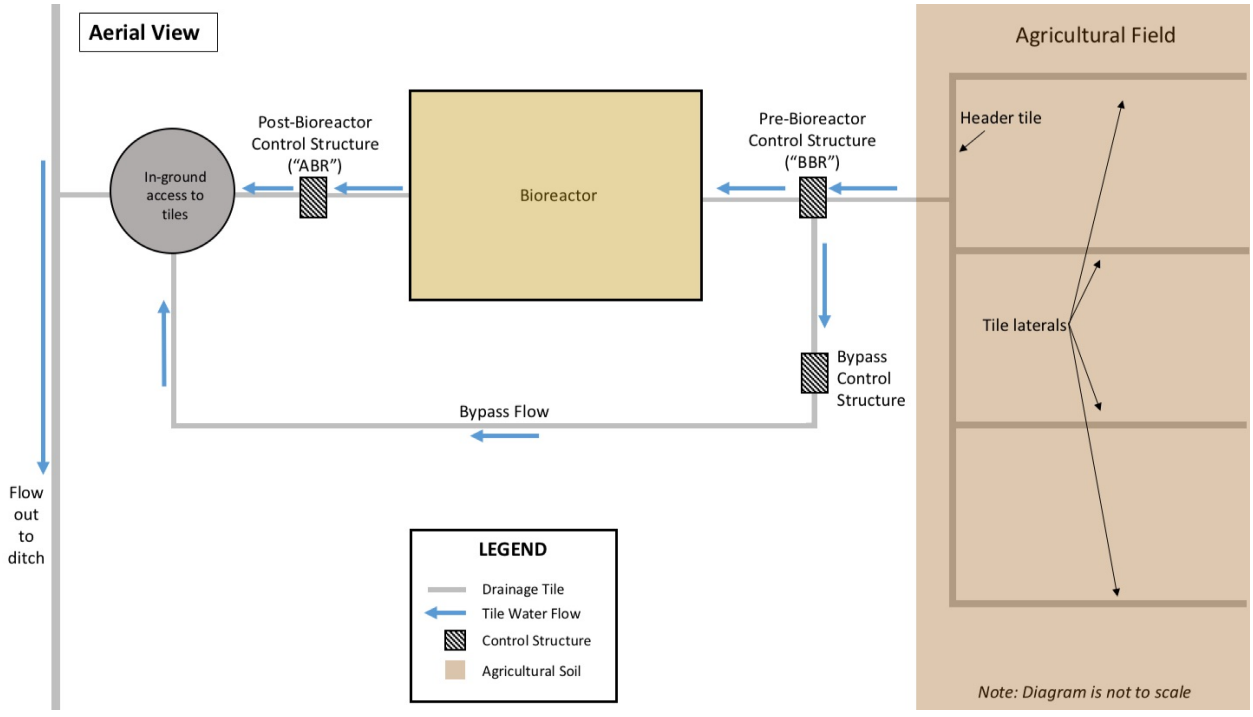

Figure 4: Illustration of a drainage management system from one of the fields including bioreactor treatment

Figure 5: Bioreactor installation partway through construction. Pre-bioreactor (BBR) control structure and bypass control structures are shown in top-right; post-bioreactor (ABR) control structure is on bottom-left. Plastic wrap is shown partially installed as well as perforated input/output tiles on opposite ends of the reactor bed.

Figure 6: Pre-bioreactor control structure (left), bypass control structure (right), and connection to bioreactor (bottom) during installation.

Figure 7: Woodchips added to a reactor bed during construction at Winchester field location.

Table 1: Percentage of Woodchips and Alum in Bioreactor Substrate

Bioreactor	% Woodchips	% Alum
T1	90	10
T2	80	20
T3	100	0
T4	100	0
T5	80	20
T6	90	10

3. Analytical Methods, Sampling, and Sample Preparation

A comprehensive fieldwork program was carried out in 2012 and 2013, including collection of soil, tile water, groundwater, plants at harvest, and soil gases during the growing season. Soil greenhouse gas fluxes were measured on average weekly, ground water was collected bi-weekly, soil was sampled monthly, and tile water was collected regularly before and after bioreactor treatment throughout 2013. During the spring of 2013, an emphasis was placed on water collection during precipitation events, and additional tile water samples were collected for analysis of $^{15}N\text{-}NO_3^-$ and dissolved N_2O concentration.

3.1 Soil

Soil samples were collected in a diagonal pattern across the fields using a hand auger at three depths: 0-15 cm, 15-30 cm and 30-60 cm. Each soil sample at each field location represents a mixture of soil from three randomly selected areas to avoid localized anomalies. The soil was kept in a cooler with ice packs and later stored in a freezer at -20 ºC. The soil was then oven-dried, ground by mortar and pestle, placed in silver capsules, and acidified with HCl to remove any carbonates. Soil samples were submitted to the G.G. Hatch Stable Isotope Laboratory at the University of Ottawa for analysis of $\delta^{15}N$ and $\delta^{13}C$ by EA-IRMS. The analysis was performed on an Isotope Cube manufactured by Elementar, Germany with a Conflo III interface connected to a Delta Advantage isotope ratio mass spectrometer (IRMS, by Thermo, Germany).

3.2 Manure

Liquid swine manure was applied to the fields by broadcasting. Manure samples were collected from the tanker trucks prior to application, stored in 500 mL plastic jars with minimal headspace and kept frozen at -20 ºC. Samples were submitted to A&L Canada Laboratories Inc. for testing of nutrients and a host of other parameters.

In preparation for isotope analysis, manure was freeze-dried using a benchtop manifold freeze dryer, samples and standards were acidified with HCl to remove any carbonates, and placed in silver capsules with a tungstic oxide catalyst (WO_3). Prepared samples were submitted to the G.G. Hatch Stable Isotope Laboratory at the University of Ottawa for analysis of $\delta^{15}N$ and $\delta^{13}C$ by EA-IRMS (see section 3.1).

3.3 Plants

Prior to harvest, plants were randomly selected and carefully removed from the soil including roots using a spade, and placed in a labelled plastic bag. Corn plants were split into three portions in 2012 (roots, cob, and remainder of plant), and five portions in 2013 (roots, cob, leaves, seeds, stem). Roots were cleaned thoroughly with water to remove traces of soil. The plant portions were then dried at 80 ºC, and ground using a ball mill to a fine powder. In 2012, plant samples were analyzed directly, whereas in 2013 the plant samples represent an average of 4 plants taken across fields T1, T3, T4, T6. The ground plant matter was placed in silver capsules, acidified with HCl to remove any carbonates, and submitted to the G.G. Hatch Stable Isotope Laboratory at the University of Ottawa for analysis of $\delta^{15}N$ and $\delta^{13}C$ by EA-IRMS (see section 3.1).

3.4 Tile water

Tile water was collected by manually activating ISCO samplers located both upstream and downstream of each bioreactor. The ISCO samplers automatically purged lines prior to pumping a pre-selected amount of sample using a peristaltic pump. Sample water was collected in pre-cleaned 1 L nalgene ISCO sampling bottles, capped and transferred to coolers containing ice packs for transport back to the lab.

In the lab, water from the 1 L ISCO bottles was split into several smaller containers for analysis. Approximately 300 mL of tile water was submitted to the Robert O. Pickard Environmental Centre (ROPEC) in Ottawa, ON for analysis of ammonia+ammonium (automated phenate method, following Standard Method 4500-NH_3), and nitrite and nitrate (ion chromatography, following Standard Method 4110B). For analysis of nitrate isotopes, approximately 40 mL of sample was transferred directly to 50 mL Corning centrifuge tubes, frozen at -20 ºC, and submitted to Isotope Tracer Technologies Inc. in Waterloo, ON. For analysis of select cations and anions, a portion of the sample water was filtered with Whitman 0.45 µm syringe filters and a total of 10 mL of the filtrate was added to each of two 15 mL Corning centrifuge tubes and frozen at -20 ºC. These samples were submitted to the University of Ottawa's Geochemistry Laboratory for analysis using an Agilent Vista ICP-AES for cations, and a Thermo Scientific Dionex ICS-2100 Ion Chromatograph (IC) for anions. Prior to submission, cation samples were acidified with 15 µL of concentrated HNO_3 as per lab submission requirements.

3.5 Groundwater

A 3 m observation well located in field T5 was used to log the depth to groundwater. Groundwater was collected from piezometers at 60 cm, 120 cm, and 200 cm depth below surface (when available) using a peristaltic pump. All piezometers were purged 24 hours prior to sampling. Equal amounts of water from each of the fields was combined into one sample to represent the front and back of the fields. Water was stored in 500 mL Nalgene bottles and kept in a cooler for transport.

In the lab, sample water was filtered with Whitman 0.45 µm syringe filters and a total of 10 mL was added to each of two 15 mL Corning centrifuge tubes for analysis of select anions and cations. Cation samples were acidified with 15 µL of concentrated HNO_3. All split samples were kept frozen at -20 ºC. Sample analysis was performed at the University of Ottawa's Geochemistry Laboratory using an Agilent Vista ICP-AES for cations and a Thermo Scientific Dionex ICS-2100 Ion Chromatograph (IC) for anions.

In addition, 300 mL of sample water was delivered to the Robert O. Pickard Environmental Center (ROPEC) laboratory for analysis of ammonia+ammonium (automated phenate method, following Standard Method 4500-NH_3), and nitrite and nitrate (ion chromatography, following Standard Method 4110B).

3.6 Dissolved Nitrous Oxide

Tile water samples were collected in May 2013 by manually activating ISCO samplers located both upstream and downstream of each bioreactor. The ISCO samplers automatically purged lines prior to pumping a pre-selected amount of sample using a peristaltic pump. Care was taken

to pump water directly into pre-cleaned 250 mL glass serum bottles, leaving no headspace, before capping each bottle with a 13 mm grey butyl stopper and covering with closed top aluminum seals. Samples were immediately crimped to avoid degassing, stored with icepacks in coolers, and refrigerated.

In the lab, approximately 3 mg of magnesium perchlorate was added to 12 mL exetainers, which were then sealed with a double layer septum and evacuated to 0.5 mbar. For each tile water sample, a total of 60 mL of water was replaced with 60 mL of helium at 1 atm. Two 30 mL syringes were used, one pre-filled with helium and the other to extract water, along with 22 gauge 1-inch needles to pierce the butyl stoppers on the serum bottles. Each sample was then shaken for 1 minute to equilibrate dissolved gases with headspace. After equilibration, 30 mL of headspace gas at 1 atm was extracted and transferred to an evacuated 12 mL exetainer.

Gas analysis was performed at Agriculture and Agri-Food Canada in Ottawa, ON with a Varian CP-3800 Gas Chromatograph (GC) featuring a CombiPal autosampler. The GC had a set injector temperature of 100 °C, and a precolumn run at 75 °C. The GC featured an electron capture detector (ECD) and a flame ionization detector (FID) – the former measured N_2O while the latter measured CO_2 and CH_4 from a single 5 mL injection. The ECD was operated at 390 °C, using Helium grade 5.0 as a carrier gas at 70 mL/min and 45 Psi. A series of standards was placed at the beginning and end of each run, and after each 10^{th} sample. All standards were overpressured to 2.5 atm prior to injection to match the samples.

3.7 Soil Gas Flux

A greenhouse gas sampling program throughout the 2012 and 2013 growing seasons resulted in a large temporal dataset of soil N_2O flux in the Winchester fields and above the bioreactors. Soil

N_2O flux was measured every 1-2 weeks (weather permitting) throughout most of 2012 and 2013, both in fields and above bioreactors, using a chamber measurement technique. Soil gas fluxes were captured at the soil-air boundary using a chamber sampling technique.

Prior to fieldwork, Labco exetainers were prepared according to Rochette and Bertrand (2008). A second septum was added on top of the existing bromobutyl septum in order to reduce leakage. The septa were used for no more than seven cycles of evacuation, air sampling and analysis, and typically less than five cycles, before replacement as per Rochette and Bertrand (2003). Approximately 3 mg of magnesium perchlorate was added to each exetainer. Batches of 30 exetainers were evacuated to 0.5 mBar using a vacuum line connected to 26-gauge needles. Exetainers were evacuated once for 8 minutes, flushed with helium gas to dilute remaining air, and evacuated a second time for 8 minutes. The vaccum line was also used to evacuate 250 mL serum bottles to 0.5 mBar in preparation for soil gas isotope sampling.

In the field, clear acrylic chambers measuring 35 cm (L) x 35 cm (W) x 15 cm (D) were inserted into the soil over each of the bioreactors and over and between drainage tiles in each of the fields. Model simulations by Hutchinson and Livingston (2001) determined that a 2.5 cm chamber depth was sufficient for 10-min deployments whereas a 13 cm depth would be necessary for a 60-min deployment; therefore, with a 40-min deployment time, chambers were inserted 10 cm below surface leaving the remaining 5 cm exposed above surface. Lids were also made of clear acrylic plastic, with a closed-cell foam gasket on the underside to form an air-tight seal with the chamber walls. The top side of the chamber lids were covered with a reflective thermo-foil material. A hole in each lid contained a #45 suba-seal rubber septum for sampling. Chamber measurements were recorded monthly in order to correct for changes in chamber area and volume throughout the season.

Gas sampling in the field took place between 10:00 and 14:00 EST to coincide with maximum soil flux. Lids were placed over the chamber collars and weighted with a brick to form an air tight seal. The first chamber gas sample was taken immediately (t=0 min), followed by samples at 6, 12, 18, and 24 minutes to capture the rate of soil gas accumulation inside the chamber. Samples were obtained using a 30 mL gas tight polypropylene syringe fitted with a 1-way stopcock and a 26G 3/8" needle. After flushing the syringe 3 times with atmospheric air, the needle was inserted through the rubber septa in the chamber lid. A full syringe (~35 mL) of chamber gas was extracted, sealed in the syringe by locking the stopcock, and transferred to a 12 mL pre-evacuated exetainer. This process is repeated for each time interval. At t=25 minutes, a pre-evacuated 250 mL serum bottle was attached to the chamber using 3/8" clear PVC tubing with a 25G 7/8" needle at each end, and left to collect for 20 minutes. Chamber gas transfer occured via suction from the negative pressure inside the serum bottle. Contamination from air inside the PVC tubing was not significant as the average internal volume was found to be 4.75 mL, or <2% of total sample volume.

Gas samples in exetainers were analyzed for concentrations of CO_2, CH_4 and N_2O as described in section 3.6.

Gas samples in 250 mL serum bottles were analyzed for $\delta^{15}N$ and $\delta^{18}O$ of N_2O at the G.G. Hatch Stable Isotope Laboratory at the University of Ottawa as per Brand (1995).

3.8 Calculations

Soil Gas flux

Gas concentration was obtained by linear regression of a calibration curve plotted using reference gas standards.

N_2O flux was calculated as per the following equation based on the ideal gas law:

$$\boldsymbol{N_2O - N\ Flux}\ (\mu \boldsymbol{g\ m^{-2}\ hr^{-1}}) = \boldsymbol{m \cdot P/(RT)}\ \cdot \left(\frac{\boldsymbol{60\ min}}{\boldsymbol{1\ hr}}\right) \cdot \left(\frac{\boldsymbol{V}}{\boldsymbol{A}}\right) \cdot \left(\frac{\boldsymbol{28.02\ \mu g\ N}}{\boldsymbol{1\ \mu mol}}\right) \qquad \textbf{Equation 3}$$

where: ***m*** is the linear slope of ppmv/min (or µL N_2O / min / L)

P is the mean atmospheric pressure in atm, during GHG sampling

R is the ideal gas constant = 0.082057 µL ▪ atm / (K ▪ µmol)

T is the in-situ chamber air temperature converted into Kelvin; (273.14 + °C)

(60min / 1 hr) is the factor to convert from minutes to an hourly basis

V is the chamber headspace volume, in litres

A is the chamber surface area, in m2

(28.02 µg N / µMol) is the factor to convert from N_2O to N basis

Dissolved N_2O

The concentration of dissolved N_2O was calculated using the concentration of gas in the headspace of each sample (see section 3.6), which was then used to estimate total dissolved N_2O per litre of sample as per Weiss and Price (1980). Pressure was assumed to be 1 atm inside each serum bottle based on the sample preparation methodology, and a salinity value of 0 was used.

4. Results

4.1 Weather and Depth to Groundwater

Available on-site data was supplemented with Environment and Climate Change Canada (ECCC) weather station data. Air temperature and atmospheric pressure are given in Figure 8, and daily precipitation and snow cover are given in Figure 9, using data from ECCC's Kemptville RCS station. Depth to groundwater and groundwater temperature were measured on-site in Winchester field T5 throughout 2013 and are shown in Figure 10.

These datasets demonstrate groundwater recharge from snowmelt in mid-January, mid-March, and at the end of March, 2013. Scattered precipitation events occurred throughout April and the first half of May, but generally the water table declined during this period. Between May 21-23, the field location received approximately 60 mm of rain, and the depth to groundwater increased from 1.0 m below surface to 0.3 m. Several rainfall events throughout June reduced the depth to groundwater to nearly 0.2 m at times. During the relatively warm and dry summer months from mid-July to mid-September, groundwater depth continued to decrease to a minimum of nearly 1.4 m below surface.

The depth to groundwater in 2012 (Figure 11) was included to demonstrate the variability in precipitation possible between years. In 2013, groundwater fell to a maximum of ~1.4 m before soil surface during the summer; whereas, in 2012, groundwater fell below the level of the deepest on-site well (~3 m) between the end of August and early December.

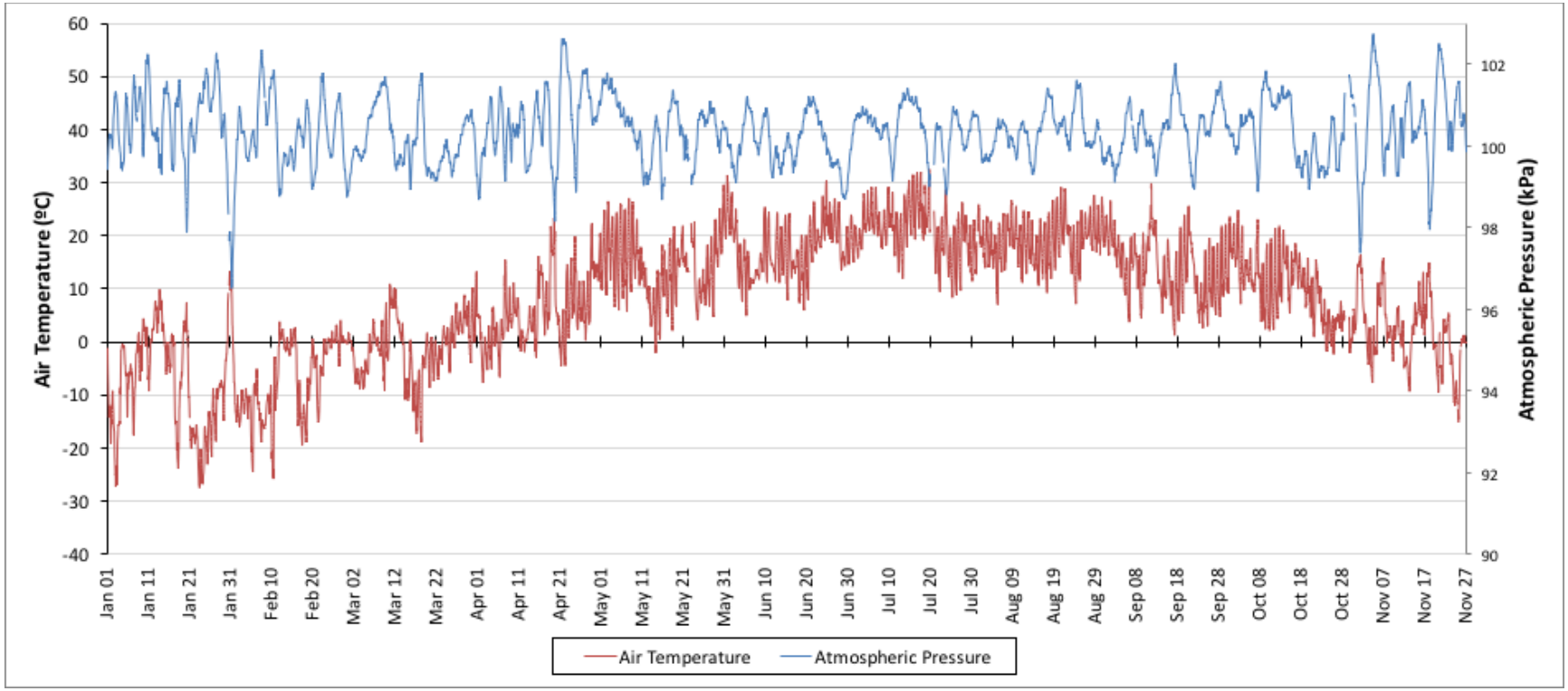

Figure 8: Air temperature and atmospheric pressure from ECCC's Kemptville RCS station in 2013.

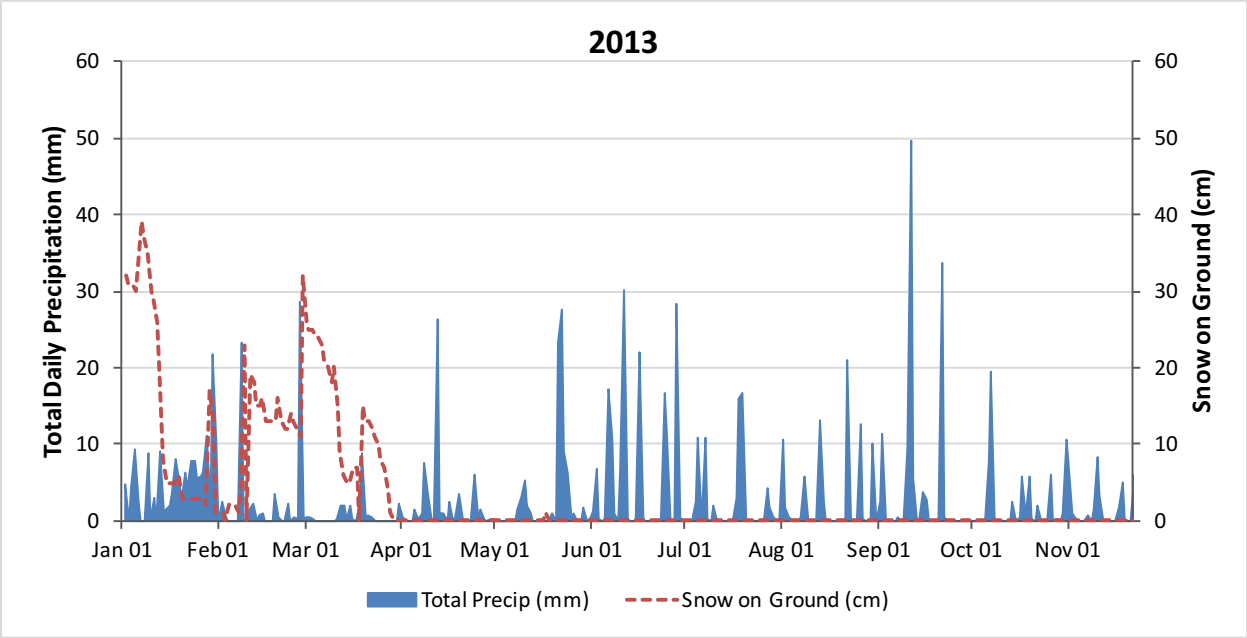

Figure 9: Total daily precipitation and snow on ground as measured at the nearest ECCC weather station (Kemptville RCS) in 2013.

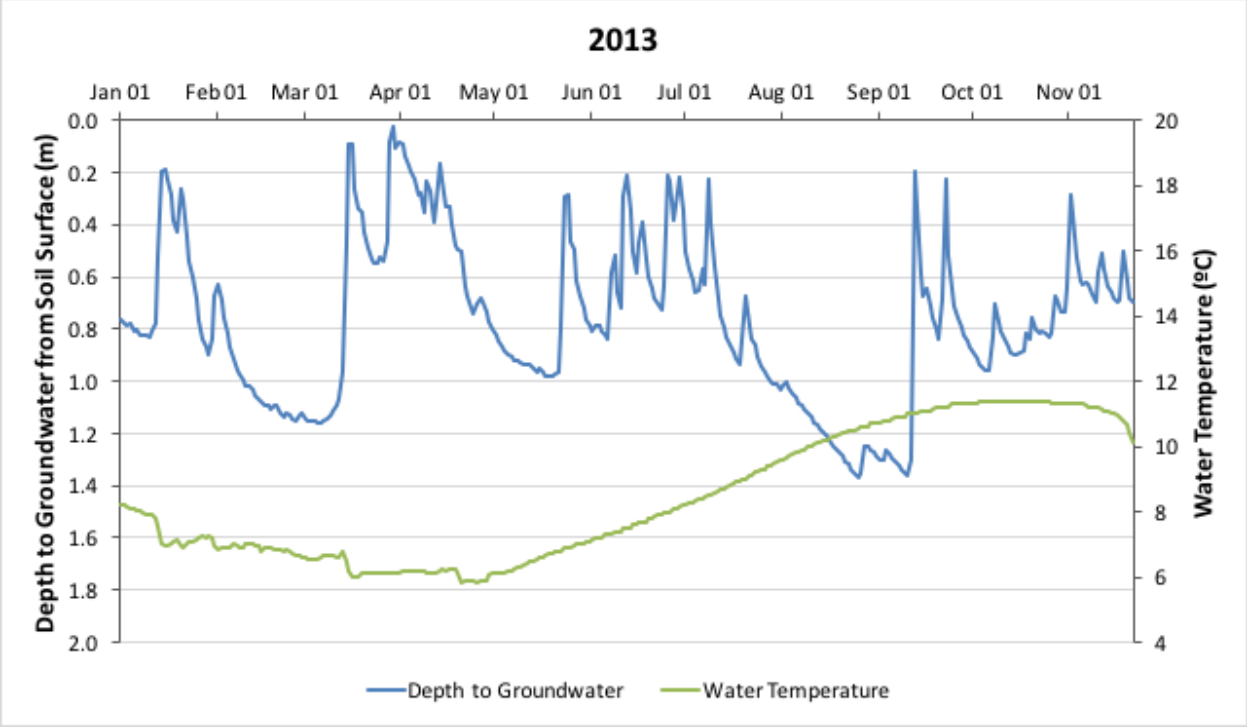

Figure 10: Depth to groundwater and groundwater temperature measured in a 3 m well in field T5 in 2013.

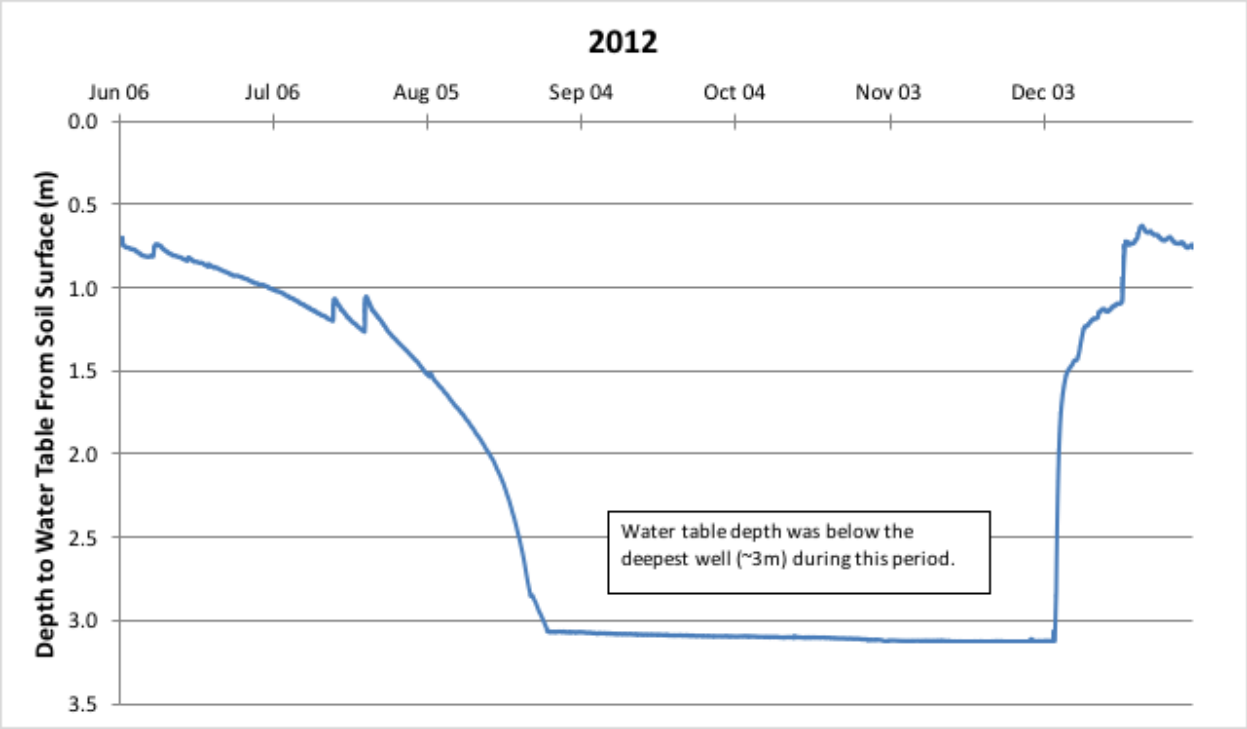

Figure 11: Depth to groundwater in summer/fall 2012 as measured in a 3 m well in field T5.

4.2 Soil N_2O Flux

The soils above the bioreactors were not tilled, did not receive fertilizer treatment, were cleared of vegetation, and were at least 10 feet from fertilizer-applied soils. Soil N_2O flux in 2012 is shown in Figure 12, and for 2013 in Figure 13.

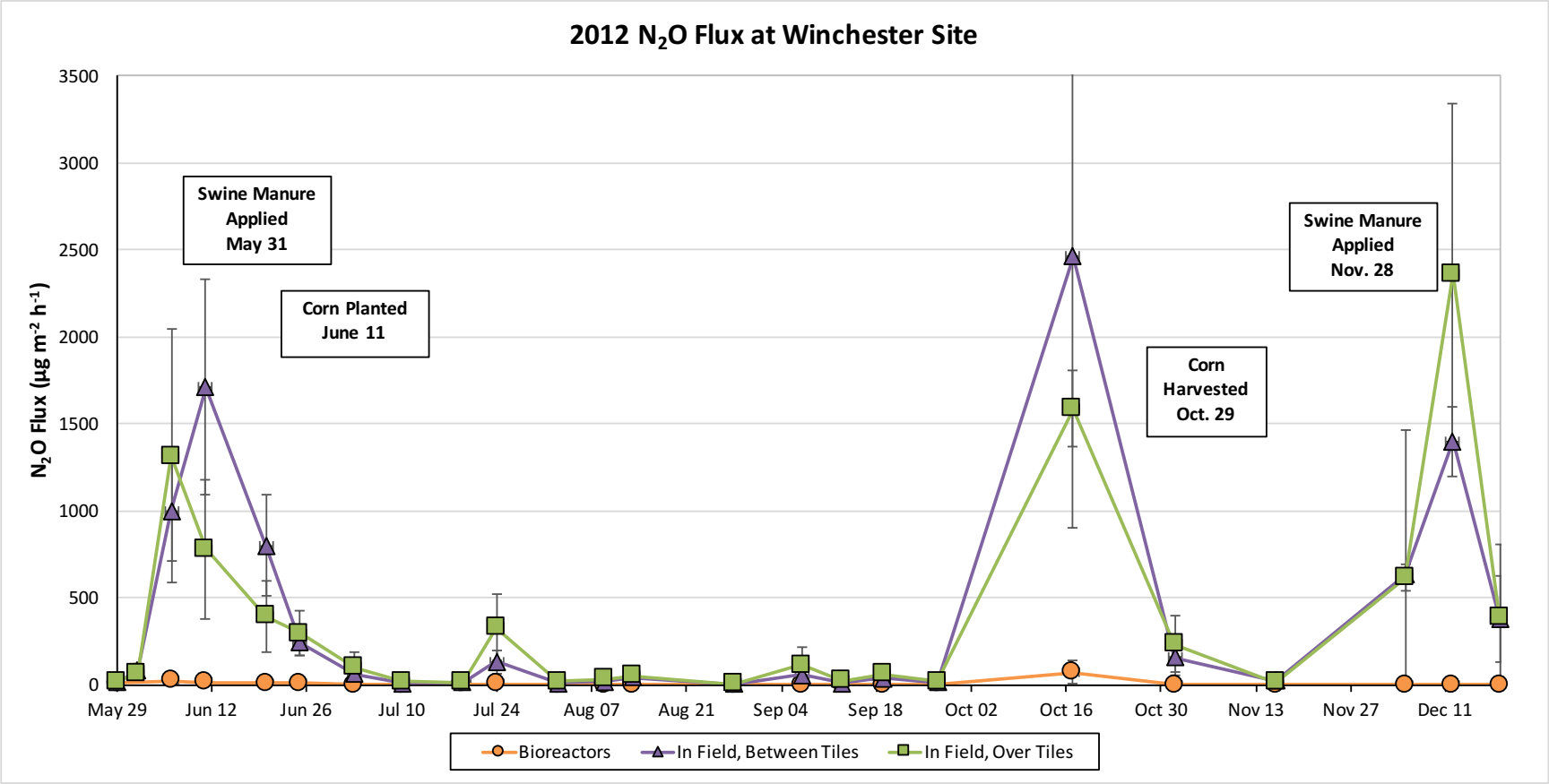

Figure 12: Soil N_2O flux measured above bioreactors, in fields between drainage tiles, and in fields above drainage tiles during 2012

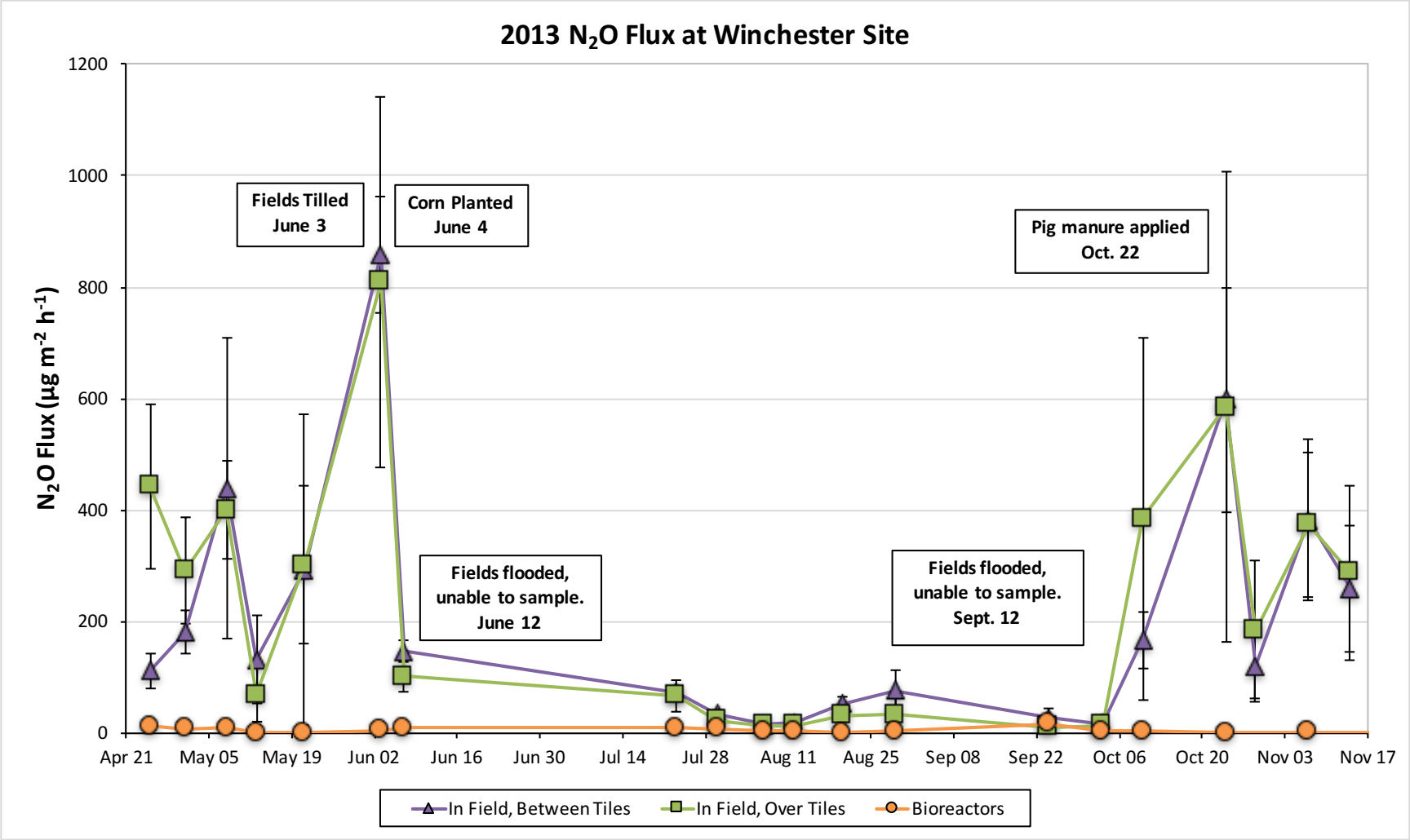

Figure 13: Soil N_2O flux measured above bioreactors, in fields between drainage tiles, and in fields above drainage tiles during 201

In 2012, there were three major flux events in the fields – early June, mid-October, early-December. The early June event followed a manure application on May 31, 2012, and produced peak flux of up to 1700 μg m^{-2} h^{-1}. The early-December flux event also followed a manure application on November 28, 2012, and produced fluxes of up to 2400 μg m^{-2} h^{-1}. The mid-October event produced fluxes of up to 2500 μg m^{-2} h^{-1}, and was not related to a manure application but was associated with increased soil moisture. This event followed rainfall during an unusually dry summer. Each data point in Figure 12 represents an average of three chamber locations. There was a large amount of variability in flux measurements during peak events due to the heterogeneity of agricultural soil and relatively small sample size. N_2O fluxes over bioreactors in 2012 were minimal to non-existent throughout the season. The largest observed fluxes above bioreactors in 2012 occurred on October 17 (71 μg m^{-2} h^{-1}), and June 6 (24 μg m^{-2} h^{-1}).

In 2013, there were two major N_2O flux events captured in the fields – one in spring around June 7 and another in the fall around October 24. Some N_2O flux occurred prior from late April to late May, ranging 100 – 400 μg m^{-2} h^{-1}. On June 7, following soil tillage and planting of corn crops, the flux in fields increased to over 800 μg m^{-2} h^{-1}. Chambers were removed from the fields between May 21 and June 4 in anticipation of tillage and planting, and later reinstalled. Data gaps in June, July and September were otherwise the result of an inability to access chambers due to flooding events in the fields. The spike in fluxes observed in October followed a manure application on October 22, 2013 and produced N_2O fluxes of up to 600 μg m^{-2} h^{-1} on October 29, 2012.

For the Spring 2013 period, measurements on June 3 and June 7 coincide with tile water flow events through the bioreactors, yet the flux observed above bioreactors on these dates averaged only 5 ±6 μg m^{-2} h^{-1} and 9 ±14 μg m^{-2} h^{-1} respectively. Additional soil flux measurement dates coincided with tile flow events during the fall of 2013, and in all cases, N_2O flux was found to be below 5 μg m^{-2} h^{-1}. The vast majority of all flux measurements above reactor beds throughout the 2013 season returned a flux less than 10 μg m^{-2} h^{-1}, with only 8 measurements between 10-30 μg m^{-2} h^{-1} and 4 at or above 30 μg m^{-2} h^{-1}. The largest single flux measurement above any one bioreactor was 57 μg m^{-2} h^{-1} and occurred on September 24, while the largest flux in spring 2013 was 50 μg m^{-2} h^{-1} and occurred April 25. N_2O flux above bioreactors were again minimal to non-existent during the 2013 season.

4.3 Applied Manure

The fields received swine manure applications of 120 kg ha^{-1} in spring of 2012, 100 kg ha^{-1} in fall of 2012, and 80 kg ha^{-1} in fall of 2013. In 2012 applications, manure was coloured with rhodamine dye in order to trace its movement through the drainage system. Samples of the manure from all applications were analyzed for a variety of parameters including ammonium concentration and percent total N (Table 2), and ammonium-N was found to account for 58-66% of total manure N (Table 3). Results for total N in manure samples from 2012 is shown in Figure 14, and demonstrates the $\delta^{15}N$ enrichment of swine manure. Total nitrogen in dry manure ranged from 3.1% in the spring application to 4.4% in the fall application, while the $\delta^{15}N$ of manure ranged between +9.2‰ and +9.5‰ for the spring application and +8.9‰ in the fall application.

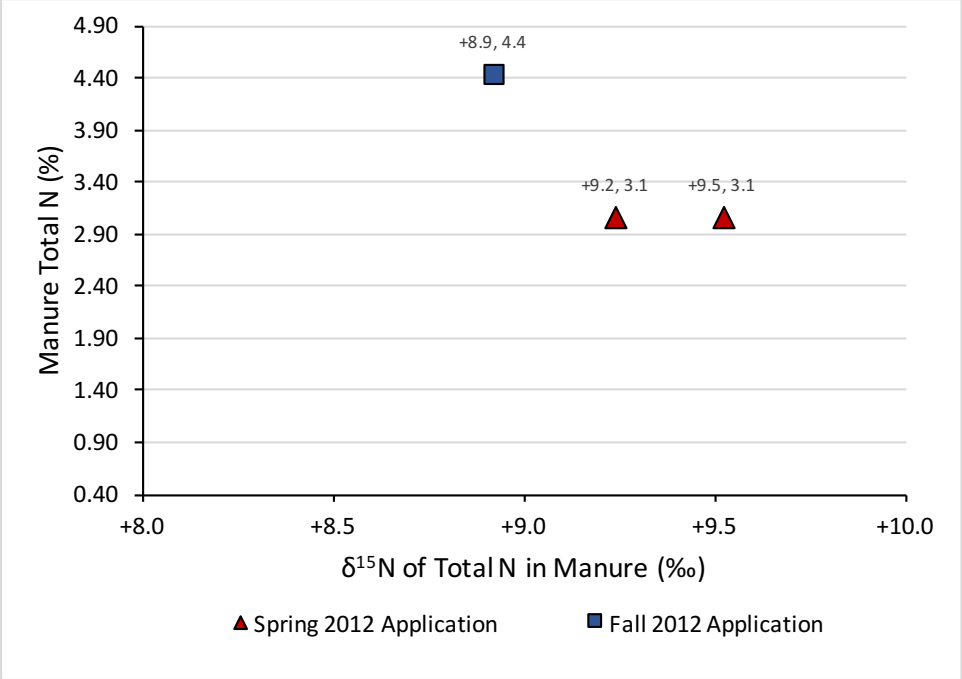

Figure 14: Manure %N and $\delta^{15}N$ of Total N from swine manure applications on May 31, 2012 and November 28, 2012. Here the %N represents the percentage of dried manure.

Table 2: Analysis of Liquid Swine Manure from Tankers Pre-Application in 2012 and 2013

Sampling date	Tanker	Bulk density (kg/m3)	Dry matter (%)	Total N (%)	NH_4-N (ppm)	TP (%)	PO_4 (%)	Organic matter (%)	S (ppm)	Total K (%)	Na (%)	Al (ppm)	Ca (%)	Fe (ppm)	Mg (%)	Mn (ppm)	Zn (ppm)
2012-05-31	1	1001	5.3	0.58	3417	0.13	0.30	4.2	18.4	0.24	0.05	34.7	0.17	132.1	0.06	27.4	71.1
2012-05-31	2	1001	5.5	0.57	3331	0.11	0.25	4.3	16.9	0.23	0.05	59.0	0.17	177.2	0.06	26.1	64.9
2012-11-28	1	1001	4.7	0.58	3661	0.13	0.30	3.5	663.1	0.34	0.07	41.1	0.15	140.0	0.07	49.8	118.0
2012-11-28	2	1002	6.2	0.74	4709	0.17	0.39	4.7	782.9	0.41	0.08	45.1	0.17	154.7	0.08	56.8	113.8
2013-10-22	1		4.0	0.59	3887	0.11	0.25	3.1	462.3	0.2	0.05	23.4	0.12	88.7	0.06	23.3	53.9
2013-10-22	2		4.1	0.59	3874	0.11	0.25	3.2	460.7	0.18	0.04	28.6	0.12	90.2	0.06	24.8	57.1

Table 3: Percentage of Total N in Tanker Manure Present as Ammonium-N

Sampling date	Tanker	Total N (%)	NH_4-N (%)	Total N as Ammonium (%)
2012-05-31	1	0.58	0.34	59
2012-05-31	2	0.57	0.33	58
2012-11-28	1	0.58	0.37	63
2012-11-28	2	0.74	0.47	64
2013-10-22	1	0.59	0.39	66
2013-10-22	2	0.59	0.39	66

4.4 Corn Plant Nitrogen

Corn crops were grown in all six Winchester fields in 2012 and 2013. Prior to harvest each year, corn plants were randomly sampled, dried, and split into plant components for analysis. In 2012, plants were split into three components (roots, cob, and remaining plant matter), while in 2013 plants were split into five portions (roots, cob, leaves, seeds, stem). Dry plant matter for 2012 plants contained an average of 1.4% N in the cob, 0.67% in the roots and 1.0% in the remainder. In 2013, plants contained an average of 1.1% N in the cob, 0.63% N in the roots, 2.1% in leaves, 0.95% in seeds, and 0.5% in the stem. All portions of the plants were found to be enriched in ^{15}N (Figure 15**)** with some differences between components and years. Roots averaged +9.0‰ in both years, while cobs increased from +7.4‰ in 2012 to +10.6‰ in 2013. The remaining plant matter (leaves, seeds, stem) was analyzed together in 2012 and had a combined isotopic signature of +5.6‰. In 2013, the seeds averaged +6.9‰, while both the leaves and stem averaged +10.1‰; therefore, all portions of the 2013 plants except roots were more enriched in ^{15}N.

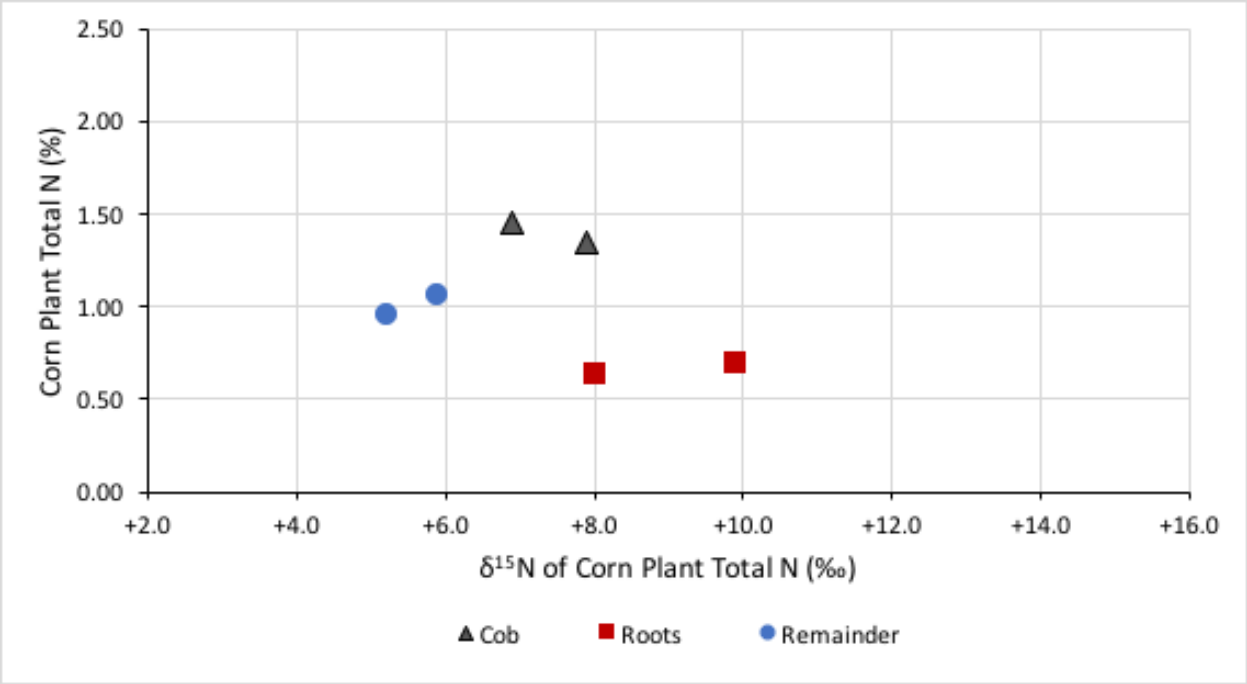

Figure 15: Total N (%) vs δ^{15}N (‰) in corn plants collected at the end of the 2012 growing season, split by plant component.

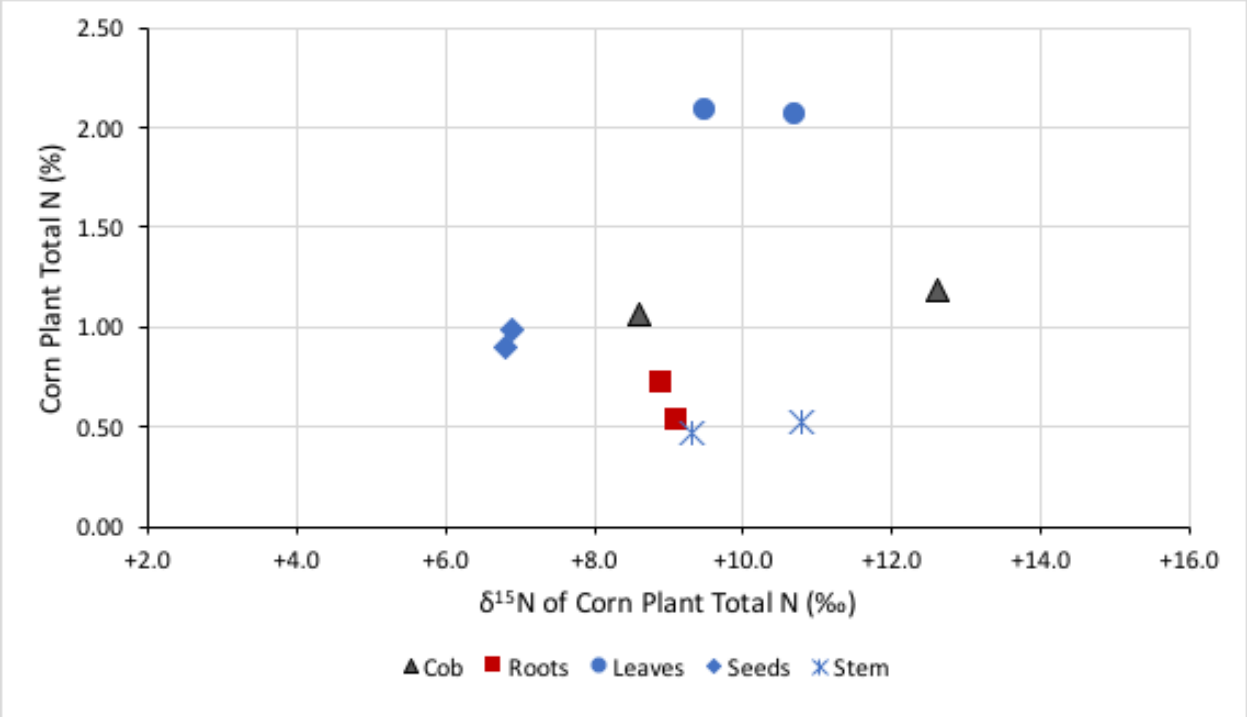

Figure 16: Total N (%) vs δ^{15}N (‰) in corn plants collected at the end of the 2013 growing season, split by plant component.

4.5 Soil Nitrogen

Soil was collected monthly on average throughout the 2012 and 2013 field seasons. Soil from the 2013 field season was selected and analyzed for %N and $\delta^{15}N$ of total N at three depths (0-15 cm, 15-30 cm, and 30-60 cm) and two field locations (between fields T1 and T2, and between fields T4 and T5). Results are shown in Figure 19 to Figure 18. May 1 soil was collected prior to tillage and planting; whereas, corn plants were growing on all other sampling dates.

The percentage of N in soil ranged from 0.16% to 0.20% at the 0-15 cm depth, 0.12% to 0.22% at the 15-30 cm depth, and 0.05% to 0.10% at the 30-60 cm depth. Attenuation of soil N was observed with depth, and is most visible when comparing soils at the 0-30 cm depths with soil at the 30-60 cm depth which contained 52% less total N on average. Some attenuation of soil N is evident over time, at the 30-60 cm depths at both locations, and at the 15-30 cm depth at the T4/T5 location; however, in other cases the trend is stable or increasing despite no additional application of fertilizer. One possible explanation is that visible fragments of crop residue were removed from soil samples during preparation for analysis. As a result, increases in soil N over time may be the result of decomposition of crop residue and incorporation with soil N.

The $\delta^{15}N$ enrichment of soil tended to decrease with depth, and is most evident when comparing 0-30 cm soils with 30-60 cm soil. The most ^{15}N depleted samples were consistently those at the 30-60 cm depth. The isotopic signature of soils at the three depths were most distinct on May 1 and tended to converge mid-season. Since the data is a measurement of total nitrogen, it represents the combination of nitrate, nitrite, ammonium, and organic N. Fluctuations in isotopic signature with depth may therefore represent a change in the relative distribution of N species by depth and/or signify reactive loss (i.e. denitrification to N_2O and N_2). At the same time, tile

drainage and growing corn plants were removing ammonium and nitrate from all three depths, decreasing the proportion of the isotope signal coming from those pools.

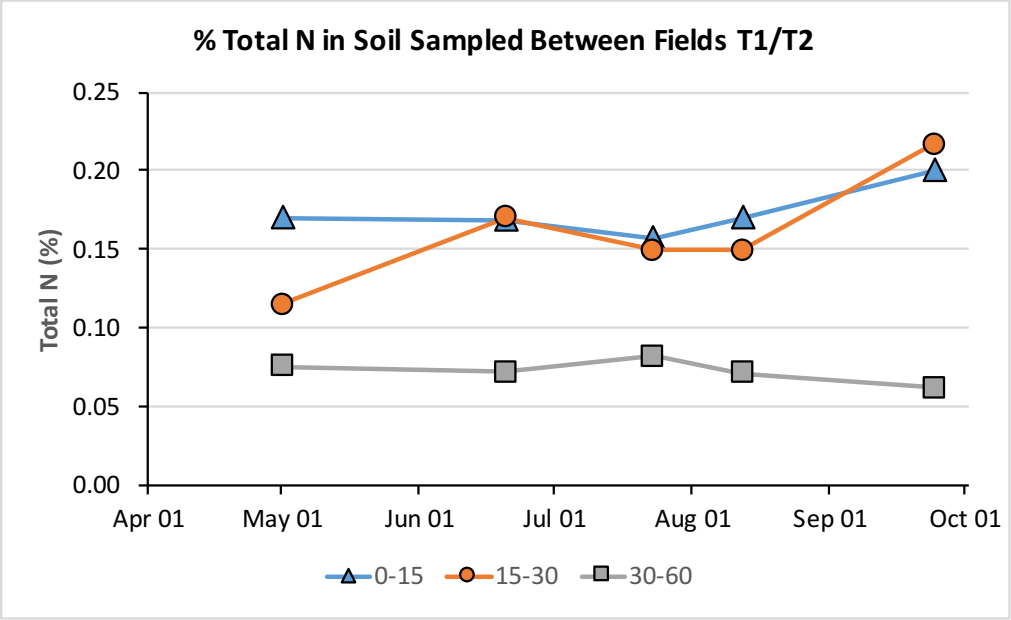

Figure 17: The percentage of total nitrogen in soil samples collected at three depths between fields T1 and T2 over the course of the 2013 growing season.

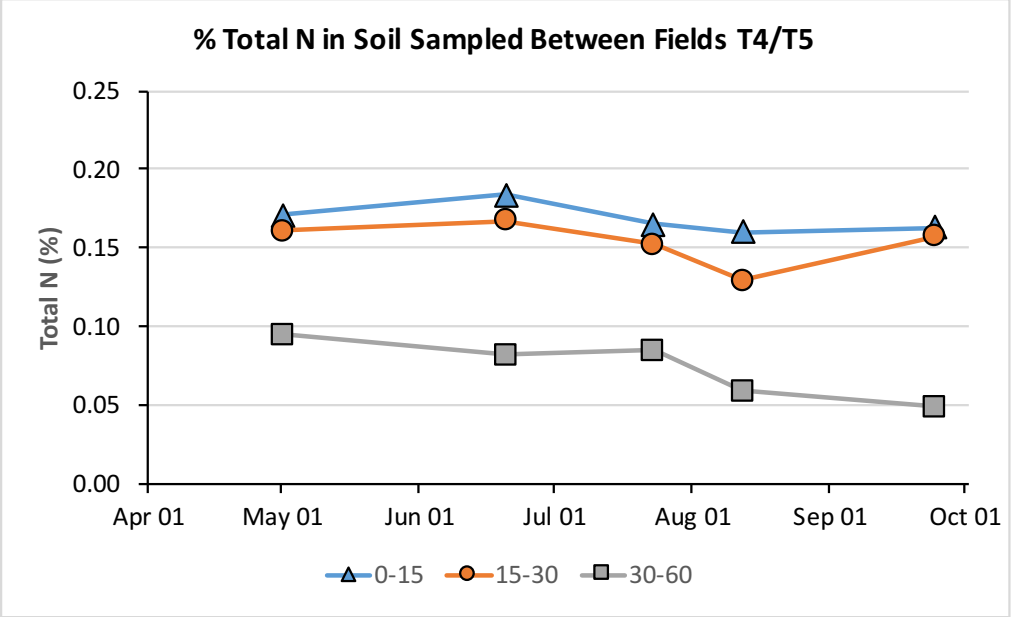

Figure 18: The percentage of total nitrogen in soil samples collected at three depths between fields T4 and T5 over the course of the 2013 growing season.

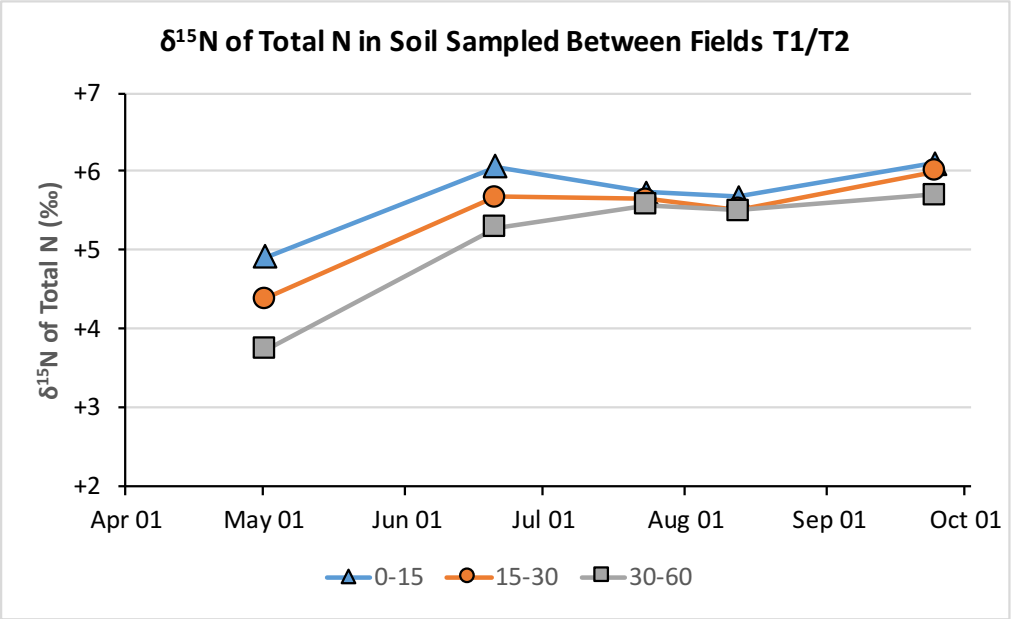

Figure 19: The $\delta^{15}N$ signature of total nitrogen in soil samples collected at three depths between fields T1 and T2 over the course of the 2013 growing season.

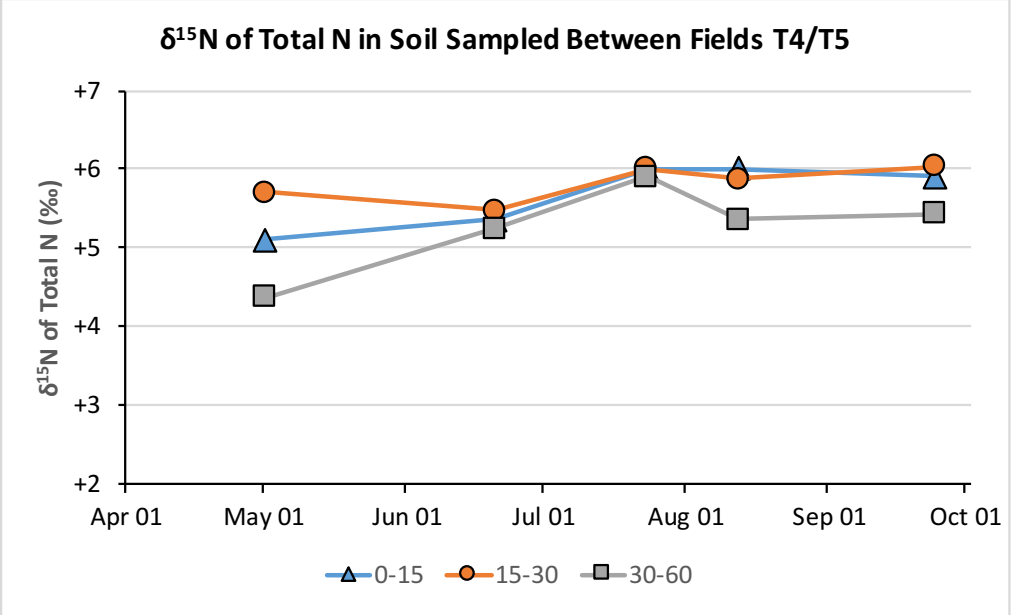

Figure 20: The $\delta^{15}N$ signature of total nitrogen in soil samples collected at three depths between fields T4 and T5 over the course of the 2013 growing season.

4.6 Nitrogen and Ions in Groundwater

Groundwater was sampled approximately every two weeks throughout the 2012 and 2013 field seasons. Pink colouration was observed in groundwater samples following the application of manure mixed with rhodamine dye in 2012, demonstrating leaching of swine manure. Samples from early 2013 were analyzed for ammonium-N and nitrate-N at depths of 2 m, 1.2 m. On May 28, groundwater recharge raised the water table sufficiently to allow for sampling at the shallowest 60 cm depth. Groundwater sampled on February 25, April 24, and May 23, contained less than 0.1 ppm NH_4-N at 1.2 m and 2 m depths, and 0.47 ppm NH_4-N at the 0.6 m depth on May 28 (Figure 21).

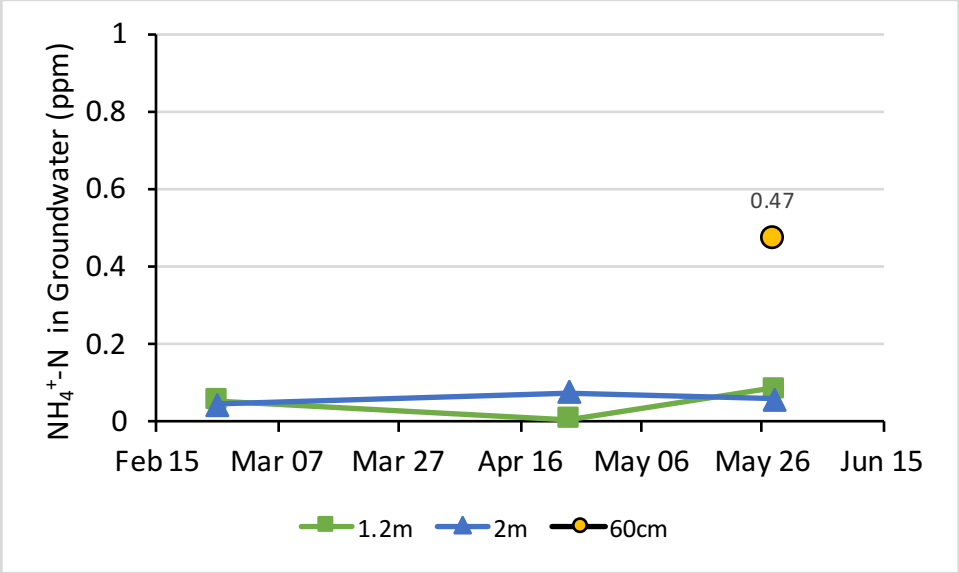

Figure 21: Average NH_4-N in groundwater at 60 cm, 120 cm and 200 cm depths during Spring 2013 leading up to the late May rainfall event

Groundwater NO_3^--N declined between February 25 and April 24 from 8.1 ppm to 5.2 ppm at 1.2 m depth, and from 2.5 ppm to 0.8 ppm at 2 m depth. From April 24 to May 23, NO_3^--N increased to 18 ppm at the 1.2 m depth but remained stable at 0.9 ppm at the 2 m depth. On May 28, nitrate was observed to increase in concentration towards the soil surface with measurements of 28 ppm, 17 ppm, and 2 ppm NO_3-N at 0.6 m, 1.2 m and 2 m depths respectively (Figure 22).

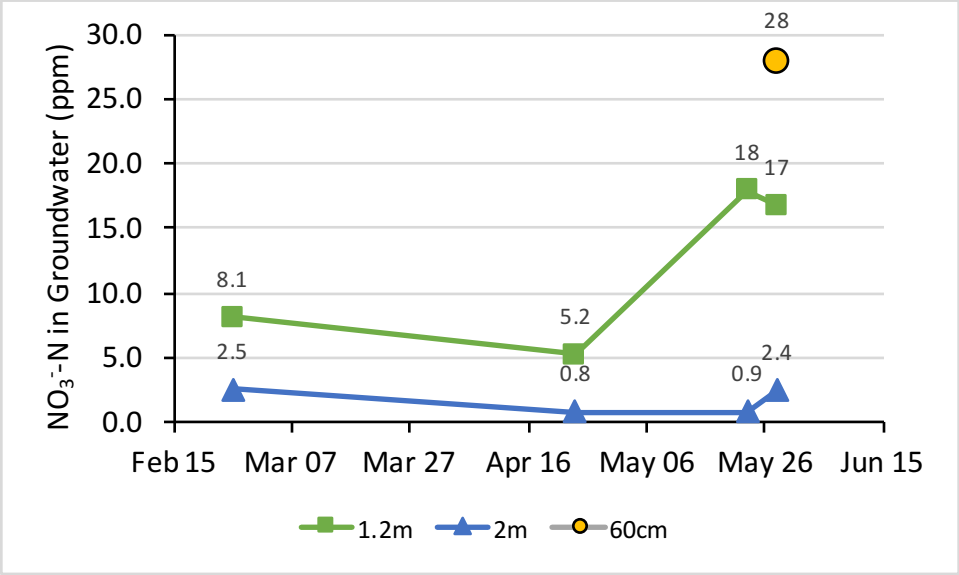

Figure 22: **Average NO_3^--N in groundwater at 60 cm, 120 cm and 200 cm depths during Spring 2013.**

A complete breakdown of major dissolved cations and anions in groundwater on May 23 is provided in Table 4. The "front" of the fields refers to locations closest to the bioreactors while the "back" of the field samples refer to groundwater collected opposite the bioreactors. The concentration of bromide was below detection limit in samples at 2 m depth.

Table 4: **Analysis of major cations and anions in groundwater taken from the front and back of the fields at 120 cm and 200 cm depths.**

Sample	Collection Date	Major Cations and Anions (ppm)										
		Ca	Fe	K	Mg	Mn	Na	S	Cl	SO_4	Br	NO_3
Front, 200 cm	2013-05-23	88.17	0.00	2.40	42.81	0.10	16.10	23.23	10.50	80.60	n.a.	6.41
Back, 200 cm	2013-05-23	77.81	0.01	2.44	39.85	0.08	13.16	16.33	13.22	55.07	n.a.	1.12
Front, 120 cm	2013-05-23	95.29	0.00	1.52	32.79	0.05	33.51	10.86	30.70	35.87	0.08	89.18
Back, 120 cm	2013-05-23	69.50	0.00	1.37	33.87	0.02	28.63	12.71	16.50	42.96	0.07	69.55

4.7 Bioreactor Treatment of Drainage Tile Water

Tile water upstream and downstream of the bioreactors was collected and analyzed for NO_3^--N and NH_4^+-N throughout 2013. Two major nitrate loading events occurred in 2013 through all six bioreactors – one in late May, and the other from mid-to late June. Both increases in nitrate followed precipitation events; however, by mid-June the fields had become flooded from the influx of rain and were no longer traversable for sampling purposes. For this reason, focus was placed on the functioning of the bioreactors during the late May rainfall event.

4.7.1 Tile Water Flow Rates

Tile water flow during the May event began at approximately 23:00 EST May 22, with water flowing into and out of all six bioreactors by 11:00 EST on May 23, and ending May 26 (Figure 23). Tile water samples were collected on May 24 between 10:00 and 11:00 EST during the second peak flow event. The flow rate of treated water exiting the bioreactors was on average

10% of the input flow rate. The remaining water (Total – Treated) was diverted through a bypass structure and mixed with the bioreactor output water. An aggressive bypass ratio of 10:1 was used in spring 2013 in order to assess the reactor substrate. Although this ratio was not typical, the impact of increasing the proportion of bypass flow should be an improvement in N removal performance due to an increase in residence time.

The flow rate of water bypassing the bioreactors was not available in May 2013; however, tile water flow captured on September 12, September 22, and November 1 includes the bypass flow (Figure 24). This fall data was included to demonstrate the correct functioning of the drainage system, in that the amount of incoming tile water from the fields was equal to the combined amount of treated bioreactor output and untreated bypass water.

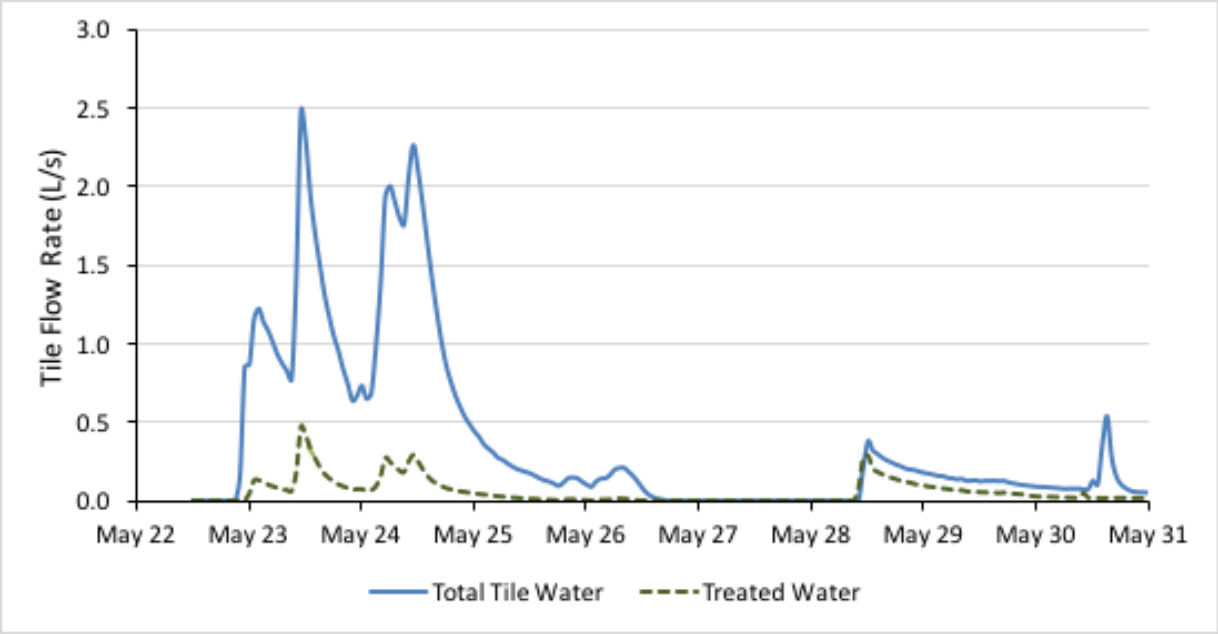

Figure 23: Sum of the average hourly tile water flow rates from all six bioreactors, measured upstream (total tile water) and downstream (treated tile water) of the bioreactors in May 2013.

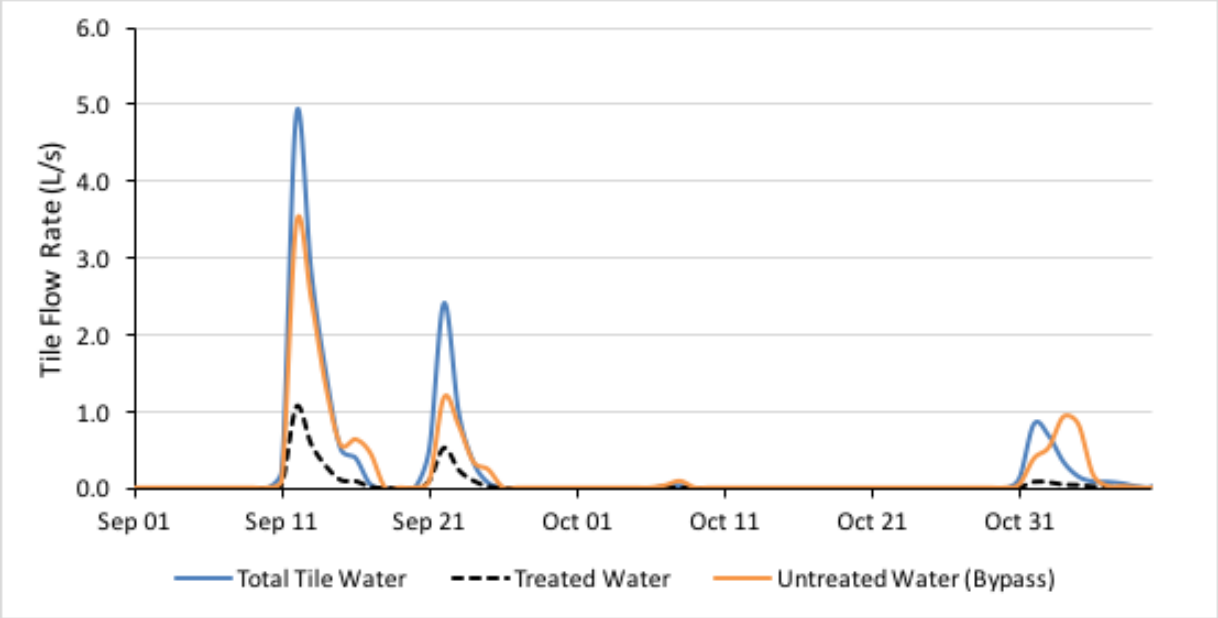

Figure 24: Sum of the average hourly tile water flow rates from all six bioreactors, measured upstream (total tile water), downstream from the bioreactors (treated tile water), and when diverted around reactor beds (untreated bypass flow) in September and October 2013.

4.7.2 Bioreactor Performance

4.7.2.1 Sample Suite #1 – Nutrients Concentrations Throughout 2013

Tile water upstream and downstream of the bioreactors was analyzed for NO_3^-N, NO_2^- and NH_4^+-N throughout 2013; results are shown in Figure 25 to Figure 30. Graphs of NO_2^- were not included as its concentrations were insignificant. Ammonium was present in minor amounts throughout 2013, generally under 1 ppm, until October 23 where NH_4^+-N briefly reached up to 47 ppm (Figure 27). These readings followed a swine manure application on October 22, 2013. A similar increase in nitrate in tile water was not observed following the manure application.

Two major surges in NO_3^--N concentration occurred in 2013 through all six bioreactors – one in late May, and the other from mid-to late June. Between May 23 and 24, NO_3^--N levels of up to 52 ppm were observed to be passing through the drainage system before falling to 2-7 ppm by May 30. The average concentrations of N species in pre-bioreactor tile water in spring 2013 are shown in Figure 31. The amount of NO_3^--N was stable throughout March and early April at between 2-5 ppm, but rose considerably by May 24 to 37 ppm. The amount of ammonium and nitrite in tile water remained under 0.5 ppm N throughout this period.

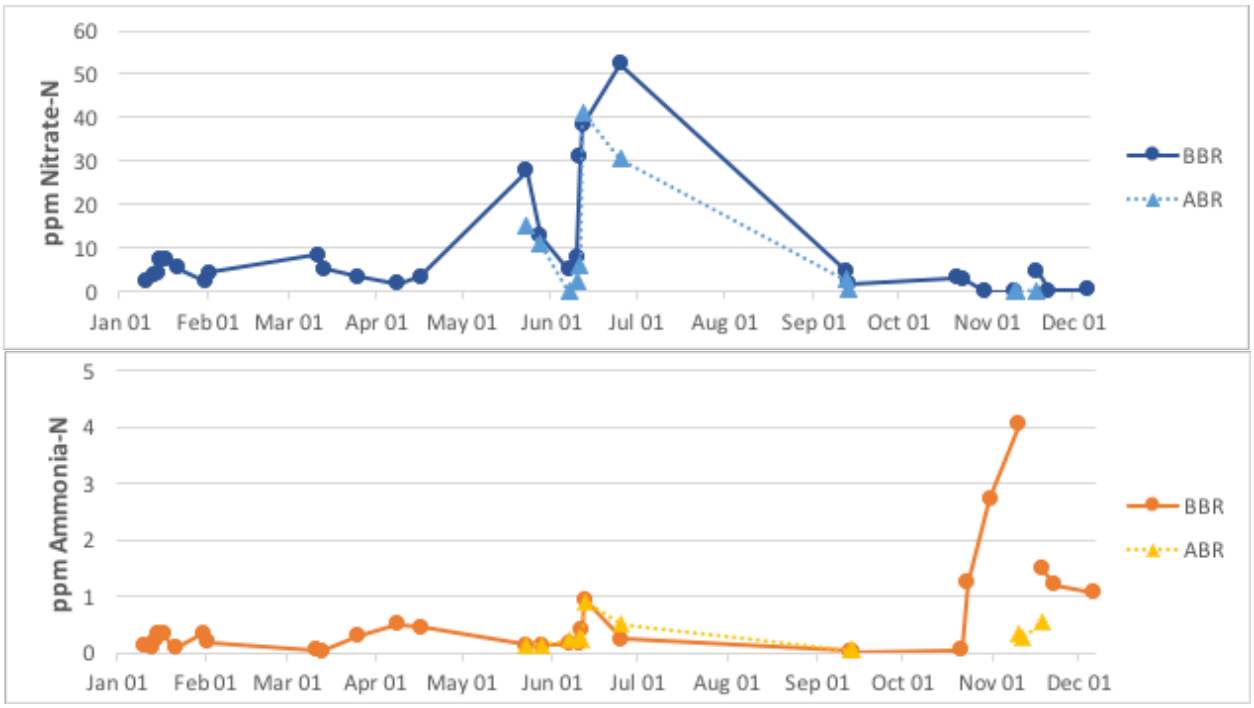

Figure 25: Nitrate and Ammonium concentrations before (BBR) and after (ABR) Bioreactor T1

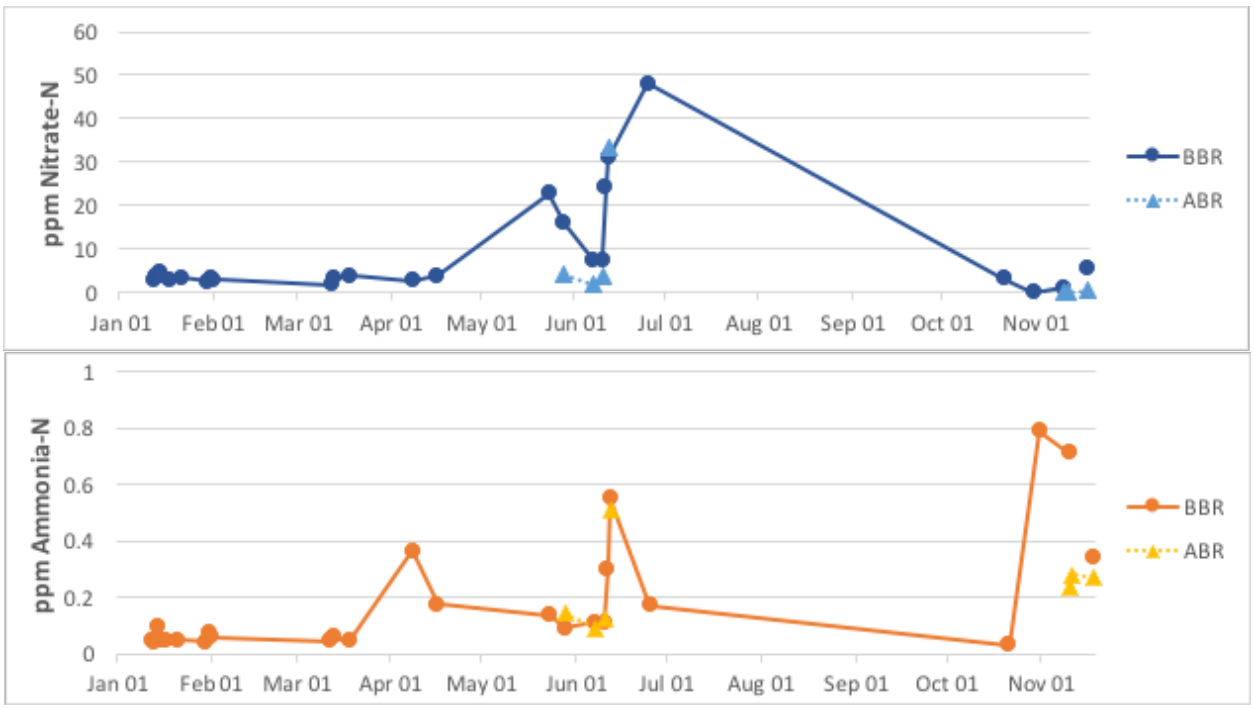

Figure 26: Nitrate and Ammonium concentrations before (BBR) and after (ABR) Bioreactor T2

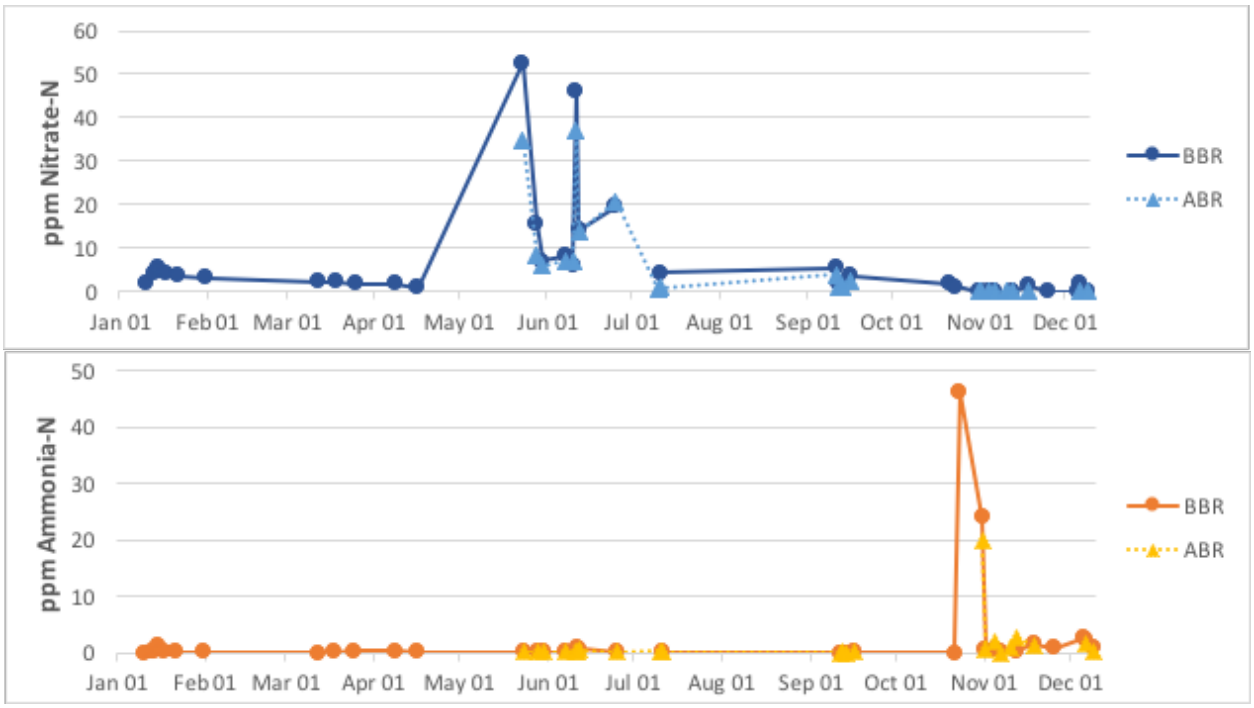

Figure 27: Nitrate and Ammonium concentrations before (BBR) and after (ABR) Bioreactor T3

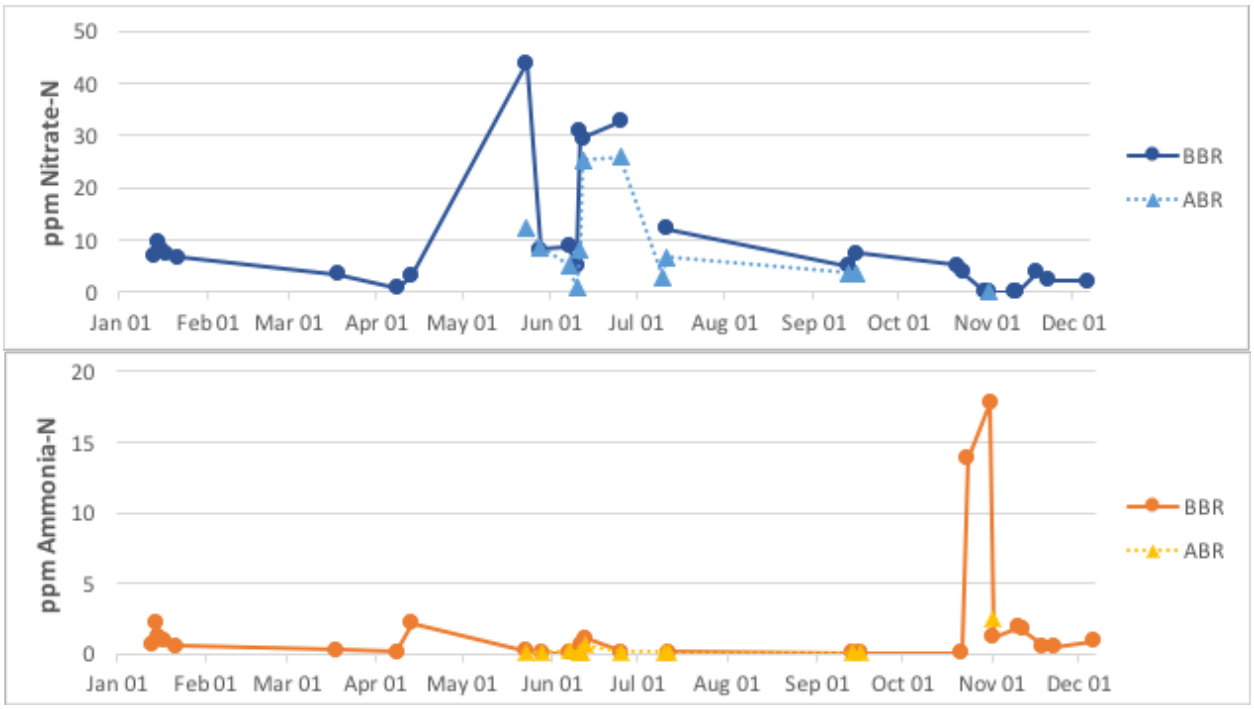

Figure 28: Nitrate and Ammonium concentrations before (BBR) and after (ABR) Bioreactor T4

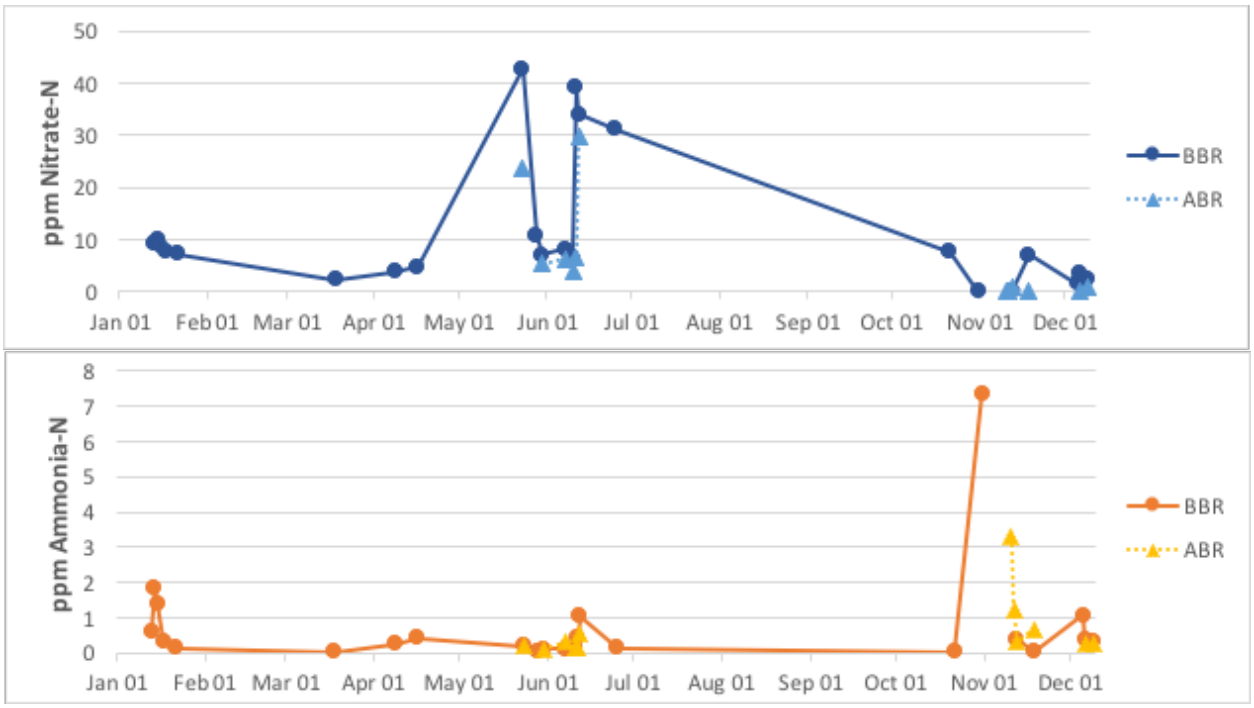

Figure 29: Nitrate and Ammonium concentrations before (BBR) and after (ABR) Bioreactor T5

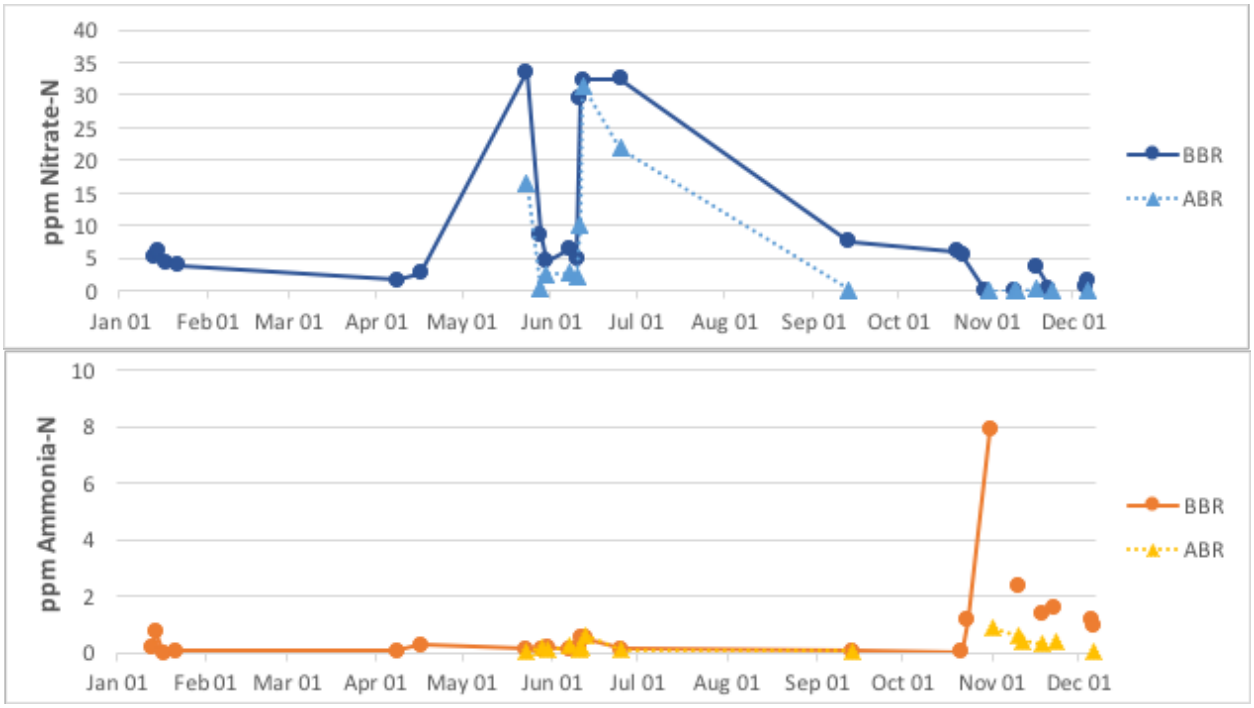

Figure 30: Nitrate and Ammonium concentrations before (BBR) and after (ABR) Bioreactor T6

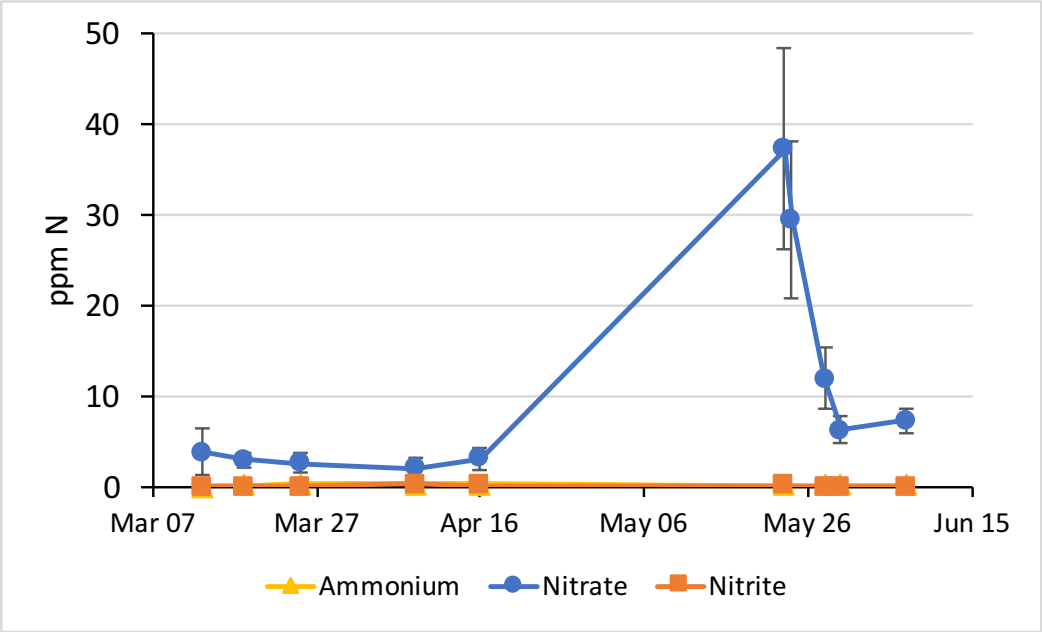

Figure 31: Average concentration of ammonium, nitrite and nitrate in pre-bioreactor tile water during Spring 2013.

4.7.2.2 Sample Suite #2 – May 24 Rain Event

A second suite of tile water samples were collected before and after bioreactor treatment on May 24. In sample suite #1, nitrate was measured on May 23; whereas, the data in this suite represents tile water on May 24 after approximately 24 hours of tile flow. These samples were analyzed for major cations and anions (Table 5) including NO_3^- (Figure 32), dissolved N_2O (Figure 33), $\delta^{15}N$-NO_3^- (Figure 36), and $\delta^{18}O$-NO_3^- (Figure 37).

The concentrations of Mg^{2+}, Na^+, Cl^-, SO_4^{2-}, NO_3^- decreased through all bioreactors with the exception of reactor T3 where their concentration remained constant.

Table 5: **Analysis of major cations and anions in tile water taken before (BBR) and after (ABR) bioreactor treatment in fields T1-T6**

Sample	Collection Date	Select Cations and Anions (ppm)										
		Ca^{2+}	Fe	K^+	Mg^{2+}	Mn^{2+}	Na^+	S^-	Cl^-	SO_4^{2-}	Br^-	NO_3^-
T1-BBR	2013-05-24	92.65	0.00	2.85	31.20	0.01	10.94	11.27	20.74	37.89	0.11	163.11
T1-ABR	2013-05-24	51.76	0.01	2.48	19.42	0.05	7.33	7.42	16.79	23.50	0.13	86.58
T2-BBR	2013-05-24	87.18	0.00	1.74	32.93	0.00	11.89	15.55	22.70	51.41	n.a.	101.67
T2-ABR	2013-05-24	56.77	0.00	1.25	19.04	0.00	6.29	6.05	10.05	21.03	n.a.	59.94
T3-BBR	2013-05-24	75.36	0.00	2.94	21.61	0.01	8.52	7.96	24.31	26.11	0.15	160.82
T3-ABR	2013-05-24	80.84	0.00	2.96	21.87	0.01	8.55	8.46	24.37	26.54	0.14	161.09
T4-BBR	2013-05-24	86.20	0.00	2.48	29.75	0.01	11.31	12.39	20.51	40.96	0.10	146.09
T4-ABR	2013-05-24	84.70	0.00	1.88	28.50	0.01	9.92	10.32	15.47	33.46	0.10	112.64
T5-BBR	2013-05-24	83.43	0.00	2.15	29.78	0.01	11.59	12.37	23.27	43.22	0.09	146.04
T5-ABR	2013-05-24	89.65	0.00	2.36	27.46	0.02	11.31	12.36	19.64	41.28	n.a.	105.28
T6-BBR	2013-05-24	73.37	0.00	1.24	27.33	0.00	10.04	10.30	21.25	33.37	0.05	66.73
T6-ABR	2013-05-24	79.15	0.01	1.06	23.18	0.01	8.05	7.54	16.25	24.60	0.06	56.02

A paired samples t-test was conducted to compare nitrate in tile water before and after bioreactor treatment. There was, on average, a 26% decrease in the concentration of nitrate between the reactor input (M=41.6, SD=12.2) and output (M=30.8, SD=12.4); t(5)=3.072, p = 0.028. There was also, on average, a 60% decrease in the concentration of dissolved nitrous oxide between the bioreactor input (M=0.085, SD=0.045) versus output (M=0.033, SD=0.029); t(5)=4.384, p = 0.007. A strong positive correlation (0.80) was found between the percent decrease of dissolved nitrate and nitrous oxide among the 6 reactors (Figure 34). Dissolved N_2O decreased by 20-40% more than nitrate through the reactors, including in reactor T3 where no decrease in nitrate was observed.

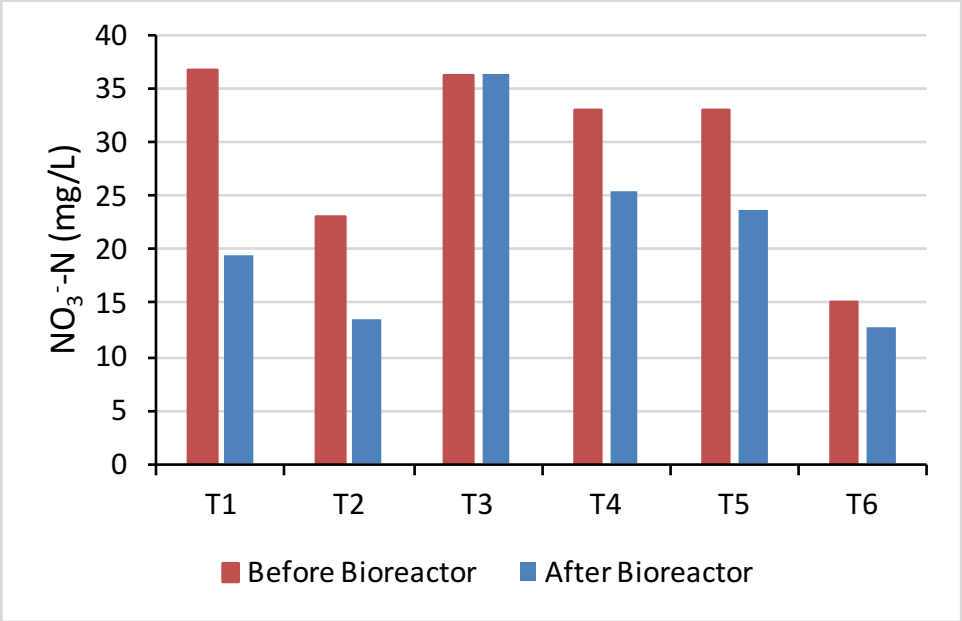

Figure 32: Nitrate-N concentration in drainage tile water before and after bioreactor treatment on May 23, 2013.

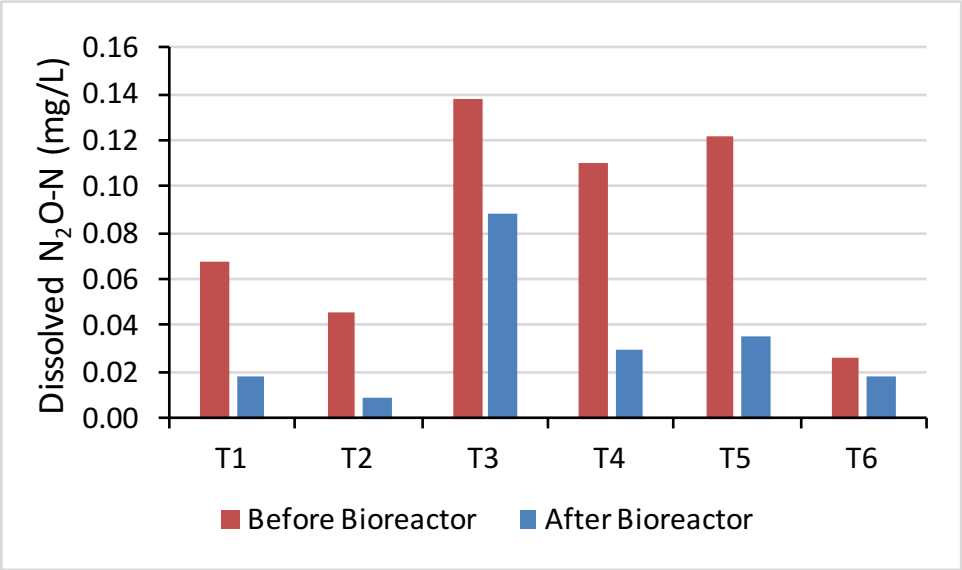

Figure 33: Dissolved N_2O-N concentration in drainage tile water before and after bioreactor treatment on May 23, 2013.

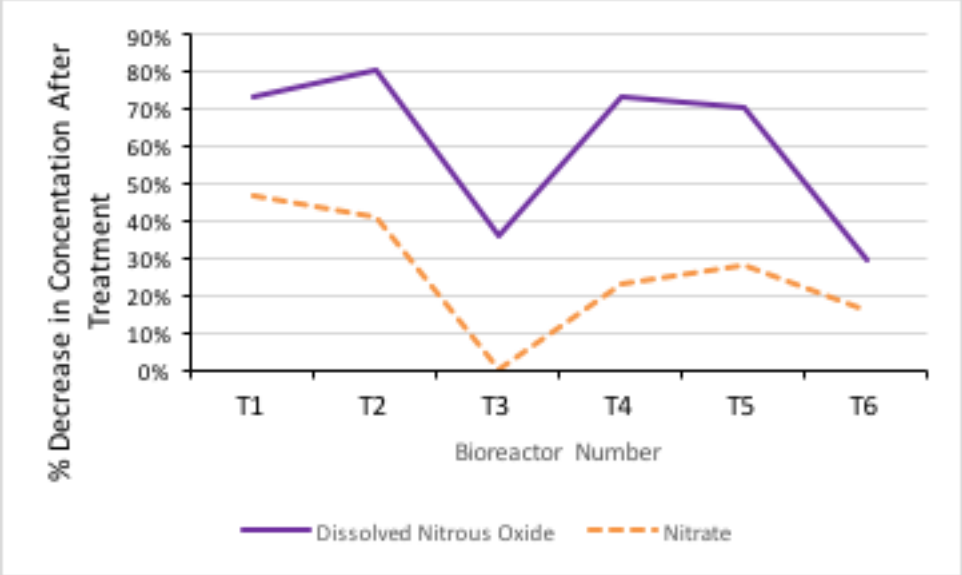

Figure 34: Percent decrease in NO_3-N and N_2O-N between bioreactor inflow (BBR) and outflow (ABR).

The average flow rate of treated water at each of the six bioreactors during water sample collection (May 24, 2013 between 10:00 and 11:00 EST), was compared against the observed percentage decrease in nitrate concentration during the same period. An inverse correlation was found (-0.81) between water flow rate and the percentage decrease in nitrate (Figure 35).

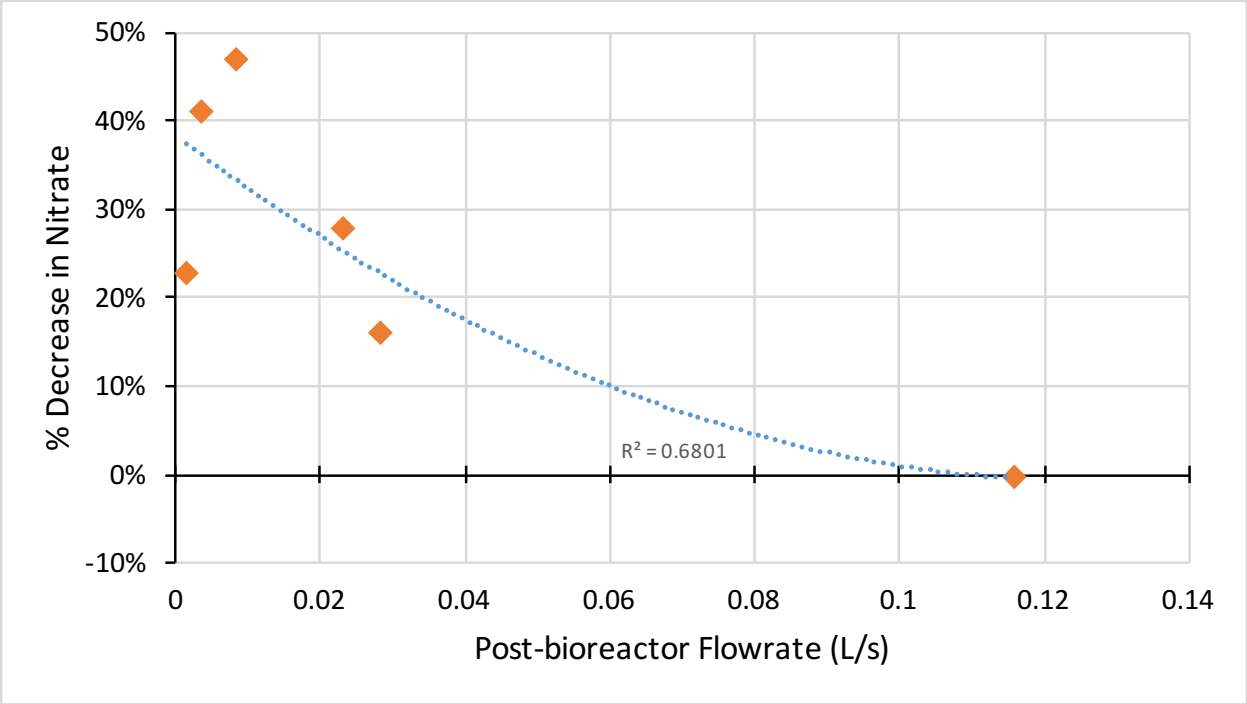

Figure 35: Relationship between the % decrease in nitrate and flowrate of bioreactor effluent at the time of sampling on May 24, 2013.

Tile water upstream and downstream of the bioreactors was examined for evidence of denitrification by measurement of $\delta^{15}N$ of nitrate (Figure 36), which becomes enriched during reactive loss, and by measurement of $\delta^{18}O$ of residual nitrate (Figure 37) which is also enriched during denitrification. Paired sample t-tests were performed to compare the isotopic enrichment of nitrate before and after passing through the bioreactors. No significant differences were observed between $\delta^{15}N$ before bioreactors (M=+11.9, SD=1.5) and after (M=+12.3, SD=12.4); t(6)=-0.522, p = 0.620, or for ^{18}O before bioreactors (M=-2.0, SD=1.5) and after (M=-1.2, SD=1.0); t(4)=-1.476, p = 0.214. These results show that significant kinetic fractionation did not occur within the bioreactor.

The amount of $\delta^{15}N\text{-}NO_3^-$ enrichment expected from denitrification was estimated using Clark (2015), the concentrations of nitrate observed before and after treatment, and a typical fractionation factor for denitrification (Equation 4). This calculation was not carried out for T3 as no decrease in nitrate concentration was observed, nor for T4 since the pre-bioreactor water was unable to be measured for $\delta^{15}N$. Results for T1, T2, T5, and T6 illustrate that denitrification would be expected to enrich nitrate far beyond what was observed (Figure 38).

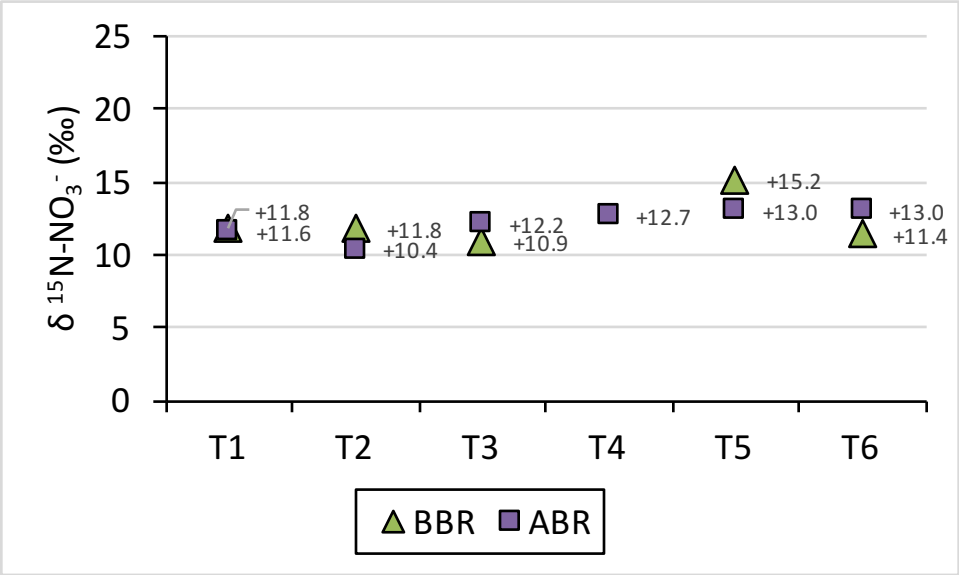

Figure 36. $\delta^{15}N$ of nitrate in tile water before (BBR) versus after (ABR) bioreactor treatment.

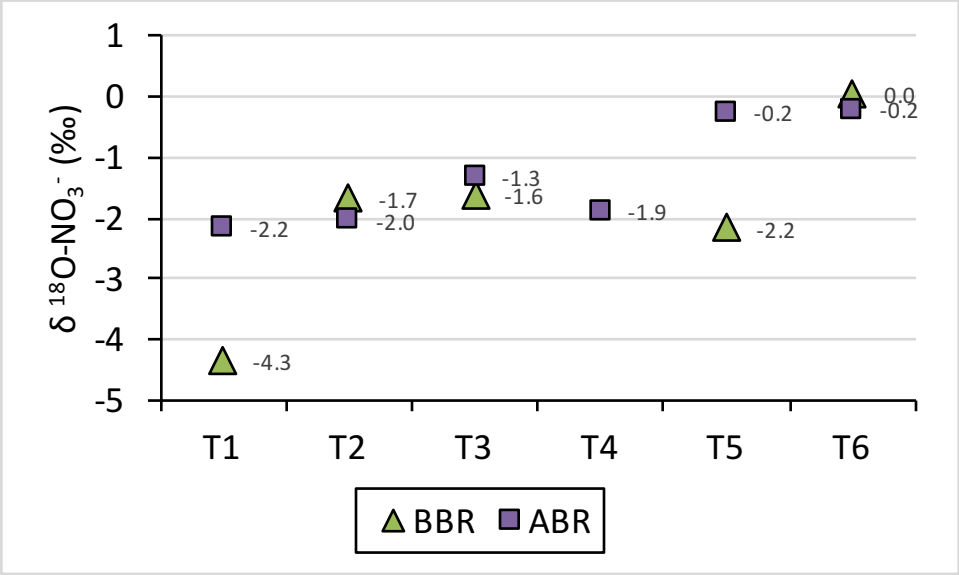

Figure 37: $\delta^{18}O$ of nitrate in tile water before (BBR) versus after (ABR) bioreactor treatment.

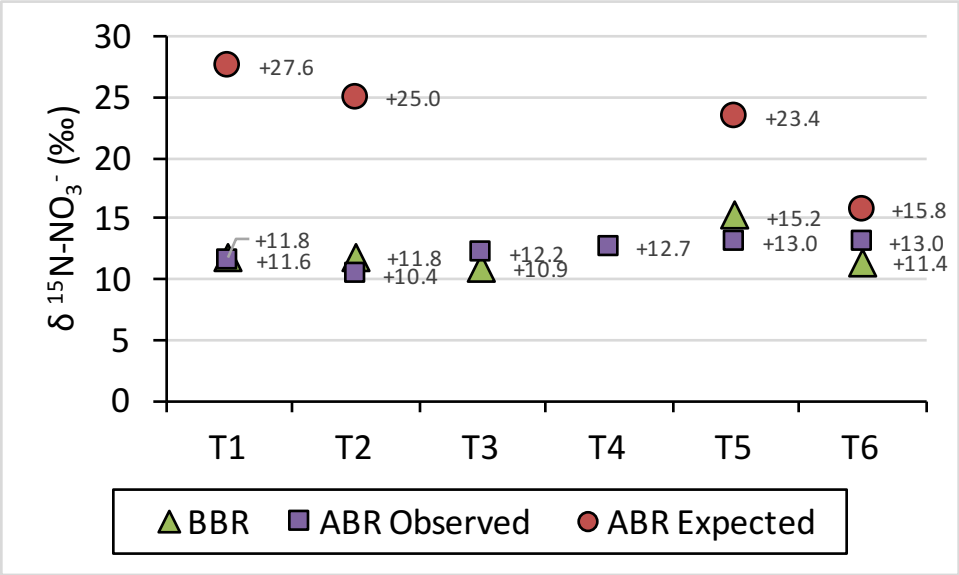

Figure 38. Expected $\delta^{15}N$ of nitrate after bioreactor treatment given the concentration change assuming fractionation from denitrification

$$E_f = E_i - [\varepsilon \cdot \ln (N_f - N_i)] \qquad \textbf{Equation 4}$$

Where:

E_f: Expected $\delta^{15}N$ of nitrate in water leaving the bioreactor (‰)

E_i : $\delta^{15}N$ of nitrate in water entering the bioreactor (‰)

ε : Enrichment factor for denitrification of nitrate (‰)

N_f : Final concentration of nitrate after passing through bioreactor

N_i : Initial concentration of nitrate before entering the bioreactor

4.7.3 Anticipated N_2O Emission from Bioreactors

Denitrification has been shown to emit a fraction of nitrate as N_2O, and if the decrease in nitrate concentration in the bioreactors on May 24 was due to denitrification, the resulting N_2O flux can be approximated based on the change in N concentration before and after treatment, tile water flow rate, reactor bed dimensions, and fraction of denitrified N emitted as N_2O. A sample calculation is shown in Equation 5 and results are provided in Table 6.

$$\mathbf{F_{N2O}} = (\boldsymbol{N_{in} - N_{out}}) \times \boldsymbol{F_{BR}} \times \left(\frac{\mathbf{1000\ \mu g}}{\mathbf{1\ mg}}\right) \times \left(\frac{\mathbf{3600\ s}}{\mathbf{1\ hr}}\right) \times \boldsymbol{A_{BR}} \times \boldsymbol{ER} \times \boldsymbol{MM} \quad \textbf{Equation 5}$$

Where:

$F_{N2O:}$ Calculated N_2O flux in µg m^{-2} h^{-1}

N_{in} : Concentration of NO_3-N in water at the bioreactor inlet in *mg/L*

N_{out} : Concentration of NO_3-N in water at the bioreactor outlet in *mg/L*

F_{BR} : Flow rate of tile water through the bioreactor in *L/s*

A_{BR} : Bioreactor area in m^2

ER : N_2O emission ratio; fraction of denitrified N emitted as N_2O

MM : Molar mass of N_2O / Molar Mass of N_2

Table 6: **N_2O Flux Expected Above Bioreactors to Account for Observed Nitrate Loss in Bioreactors on May 24, if Attributed to Denitrification.**

Bioreactor	N_2O Emissions at Four Different N_2O:N_2 Production Ratios ($\mu g\ m^{-2}\ h^{-1}$)			
	1%	5%	10%	20%
T1	15381	76905	153811	307621
T2	1692	8459	16917	33834
T4	1104	5521	11042	22084
T5	4292	21462	42924	85849
T6	743	3715	7430	14860

*NOTE: Bioreactor T3 was not included in this calculation as there was no decrease in nitrate observed.

The concentration of dissolved nitrous oxide was observed to decrease through the bioreactors (Figure 33); whereas, denitrification would be expected to produce N_2O. In order to evaluate the possibility of degassing and upward diffusion through the soil surface as a means for N loss, the resulting N_2O flux was approximated based on the change in N_2O concentration before and after treatment, tile water flow rate, and reactor bed dimensions. A sample calculation is shown in Equation 6 and results are provided in Table 7. The calculation of potentially degassed N_2O is dependent on flow rate; for example, dissolved N_2O in water samples from fields T1 and T2 was observed to decrease by 0.05 and 0.04 mg/L respectively; however, the bioreactor flow rate at T2 was one fifth that of T1, leading to a much smaller expected flux. This is a conservative estimate as it does not consider any N_2O produced in the bioreactor by denitrification, and the flow rates were below average on May 24, with only ~10% of water treated. Throughout the remainder of the season, the bioreactors typically received ~20% of total flow.

The expected fluxes were 1-2 orders of magnitude larger than those observed in chamber measurements throughout 2012 (Figure 12) and 2013 (Figure 13). This suggests that the primary mechanism for loss of dissolved N_2O was not degassing.

$$F_{N2O} = (N_{in} - N_{out}) \times B_{flow} \times \left(\frac{1000\ \mu g}{1\ mg}\right) \times \left(\frac{3600\ s}{1\ hr}\right) \div B_{area} \times MM \qquad \textbf{Equation 6}$$

Where:

F_{N2O}: Calculated N_2O flux in µg m^{-2} h^{-1}

N_{in} : Concentration of dissolved N_2O-N in water at the bioreactor inlet in *mg/L*

N_{out} : Concentration of dissolved N_2O-N in water at the bioreactor outlet in *mg/L*

B_{flow} : Flow rate of tile water through the bioreactor in *L/s*

B_{area} : Bioreactor area in m^2

MM : Molar mass of N_2O / Molar Mass of N_2

Table 7: **N_2O Flux Expected Above Bioreactors if the Observed Dissolved N_2O Loss on May 24 was Due to Degassing**

Bioreactor	Expected N_2O
	µg m^{-2} h^{-1}
T1	4395
T2	667
T3	8418
T4	1853
T5	3999
T6	235

5. Discussion

5.1 Nitrogen Movement

The optimum N content and composition of agricultural soil can vary based on crop type. Corn crops are nitrogen intensive, requiring a high relative proportion of N to other nutrients (Bundy, 1998). Liquid swine manure contains a large fraction of N as ammonium-N on the date of application, allowing corn N requirements to be met without over-applying other nutrients such as P or K. By comparison, liquid dairy manure averages 42% ammonium-N and solid hog manure contains on average 26% ammonium-N (OMAFRA, 2009).

5.1.1 2012 Manure Applications

Swine manure was applied to Winchester soils twice in 2012, once in the spring (May 31) at a rate of ~120 kg N ha^{-1} and again in the fall (November 28) at a rate of ~100 kg N ha^{-1}. The spring manure contained 0.58% total N (Table 2), of which 58% was ammonium (Table 3), and its average $\delta^{15}N$ enrichment was +9.4‰ (Figure 14). On October 22, 2012, soil from 15-30 cm depth was found to contain 1.61 ppm organic N, 8.3 ppm annomium-N, 0.05 ppm nitrite N, and 23.1 ppm nitrate-N (Coyotzi, 2016), thus after the 2012 growing season most of the NH_4^+ had been converted to NO_3^- and there was still a considerable amount of plant-available N in the soil. On November 28, 2012, swine manure slurry was again applied to soil to study the effects of late fall manure application. The manure was applied by broadcasting as soil temperatures approached 0 ºC and with some snow accumulation; however, soil was not tilled. The manure contained 0.66% total N, of which 63% was in the form of ammonium-N, and its average $\delta^{15}N$ enrichment was +9‰.

The percentage loss of ammonia varies depending on several factors including air temperature and wind speed. When liquid swine manure is applied by surface spreading, up to 90% of TAN (total ammoniacal nitrogen, comprised of $NH_3 + NH_4^+$) may be volatilized within 96 hours of application with a 20 ºC average air temperature, and 60% with a 10 ºC average air temperature, with ~20 km/h winds (Huijsmans, 2003). The majority of ammonia volatilization usually occurs within 24 hours of application (Meade et al., 2011). The effects of sub-zero air temperatures and snow cover on ammonia volatilization from applied swine manure have not been well documented, but a reduced amount of volatilization may have occurred leading to ^{15}N enrichment of ammonia near the soil surface.

The manure applications were followed by large soil N_2O fluxes of up to 1700 $\mu g\ m^{-2}\ h^{-1}$ for the spring application and up to 2400 $\mu g\ m^{-2}\ h^{-1}$ after the fall application (Figure 12). There are many possible reaction pathways that can occur in soil to produce N_2O (Butterbach-Bahl et al., 2013), but it is generally accepted that N_2O emissions from agricultural soils are the product of nitrification and denitrification (Environment Canada, 2015b; Maag and Vinther, 1996). Water content of soils is the most important factor affecting N_2O emissions (del Prado et al., 2006). The applied manure served to increase available carbon in nitrate-rich soil and was comprised of less than 6% dry matter (Table 2) therefore boosting soil moisture during infiltration of the liquid manure fraction. Soil moisture, carbon availability and nitrate are all parameters that enhance the denitrification potential of soil, and in addition, field studies have demonstrated increased denitrification in finer textured soils (Aulakh et al., 1992). A wide variety of denitrifiers were identified in Winchester soil samples, including *Burkholderia, Nitrososphaera, Ralstonia* and *Janthinobacterium* (Coyotzi, 2016). Research on silt loam soils in the cornbelt has shown that

denitrification can remove 1-5% of soil nitrate per day, depending on soil temperature, when soils are saturated with water (Verhallen, 2004).

5.1.2 Sources of Plant-Available N in 2013

No manure application occurred in spring 2013. The main sources of N in the fields for the 2013 growing season were the two 2012 manure applications, as well as decomposing corn crop residue from the previous year.

In plants, N is found in chlorophyll and plant proteins and the total N of plants will primarily measure organic-bound N. Whereas leguminous plants have the ability to obtain a portion of their N input through fixation of atmospheric N (Graham and Vance, 2003), corn plants do not and absorb N entirely through root uptake. As a result, all organic-bound N in the plant reflects the available nitrogen available to the plant roots during growth. The 2012 corn plants were grown from soil N originating from background N plus one (spring 2012) manure N application; whereas, the 2013 plants were grown from at least two manure applications (spring 2012 and fall 2012), and previous crop residues including the 2012 corn crop.

Corn crop residue includes mainly leftover roots and stalk. In the 2012 plants, corn root $\delta^{15}N$ was found to be between +8‰ and +10‰, and the remainder of the plant (stalk, leaves, seeds) averaged between +5‰ and +6‰ combined. This is similar to the manure and overall soil N from which the plant grew, and therefore decomposition of corn residue during the 2013 season would not introduce drastically enriched or depleted N to the soil.

5.1.3 2013 Soil

Total N from soil samples taken throughout the 2013 growing season contained on average 50% more total N within 30 cm of the soil surface than at 30-60 cm depth, indicating attenuation of N with depth (Figure 17 and Figure 18). In May, soil was more enriched in ^{15}N towards the surface due to volatilization of ammonia, and reactive loss by nitrification and denitrification (Figure 19 and Figure 20). Nitrification of NH_4^+ in aerobic soils near the surface generated relatively ^{15}N-depleted NO_3^-, which was more mobile and leached downward increasing the relative proportion of nitrate in total N at the 30-60 cm depth.

Soil texture can also affect the downward movement of leached nitrate in soil. Research in the cornbelt suggests that for silt loam soils, 1 cm of water enteing the soil may only move nitrate downwards 6 cm, whereas with a sandy loam the same amount of water may move nitrate 12 cm (Verhallen, 2004).

Enrichment of ^{15}N-total N in soil at the 30-60 cm depth between May and June (Section 4.5) coincided with a slight decrease in concentration and soil N_2O fluxes between 100-800 $\mu g\ m^{-2}\ h^{-1}$ (Section 4.2), indicating the presence of denitrification. The enrichment of ^{15}N-total N continued from June to July; however, from late-July to early-August, the trend reversed and soil total N became more depleted in ^{15}N. The concentration of total N decreased most sharply through this period. During the hot and dry summer months, the water table declined (Figure 10) and the proportion of nitrate in soil probably decreased as nitrate migrated downward. Since nitrate had become enriched in ^{15}N from May to July during denitrification, the resulting effect of its removal on $\delta^{15}N$-Total N was depletion of ^{15}N.

5.1.4 2013 Groundwater and Tile Water

The amount of ammonium-N in groundwater was less than 0.5 ppm throughout the spring at all depths (Figure 21). On the other hand, groundwater contained up to 28 ppm of nitrate and displayed attenuation with depth (Figure 22). This demonstrates nitrification of manure NH_4^+, and leaching of nitrate. The amount of nitrate at 1.2 m depth more than tripled from 5.2 ppm to 18 ppm between April 24 and May 23 indicating an influx of leached nitrate. Between May 23 and May 28, the amount of nitrate at 1.2 m decreased slightly while nitrate at 2 m depth increased, demonstrating the downward movement of leached nitrate.

Drainage tiles were located approximately 1 m below the soil surface, collecting water and moving it towards the pre-bioreactor control structure. Tile water nitrate and ammonium was measured regularly throughout 2013, both before and after bioreactor treatment at all six bioreactors (Figure 25 to Figure 30). There were two periods where tile water contained above-average amounts of nitrate, one in late May and another in mid-June. During both events, the concentration of NO_3^--N in pre-bioreactor tile water reached as high as 52 ppm, and in all cases, less nitrate exited the bioreactor than went in. These events are discussed in section 5.2.

Ammonium-N remained below 3 ppm in all drainage tiles throughout the year with the exception of a brief period beginning October 23 where NH_4^+-N rose sharply, reaching as high as 47 ppm (Figure 27) following a liquid swine manure application on October 22. A similar increase in nitrate was not observed, indicating that a fraction of the manure NH_4^+-N quickly leached and passed through the drainage system without undergoing nitrification. Generally, less ammonium exited the bioreactor than entered during this event. This may have been the result of simultaneous nitrification and denitrification inside the bioreactor; however, reactor beds are low

oxygen environments optimized for denitrification where nitrification is unlikely to occur. In addition, bioreactors typically remove a large fraction but not all incoming nitrate, and consequently some increase in bioreactor nitrate would be expected. Alternatively, mixing may have occurred between the influx of ammonium-rich tile water and pre-existing bioreactor water, especially considering that ammonium concentrations of this magnitude were not observed prior to October 23.

5.2 Bioreactor Performance During a Heavy Rainfall Event in Late May 2013

5.2.1 Tile Water Flow

Two major tile flow events occurred in 2013 bringing elevated levels of nitrate through all six bioreactors. One event occurred in late May, and the other from mid-to late June. Both followed precipitation events; however, by mid-June the fields had become flooded from the influx of rain and were no longer traversable for sampling purposes. For this reason, focus was placed on the functioning of the bioreactors during the late May rainfall event.

The May rain event occurred between May 21-24, 2013 and deposited 23 mm of rainwater on the 21st, 28 mm on the 22nd, 9 mm on the 23rd and 6 mm on the 24th of May, for a total of 66 mm of rain water (Figure 9). Tile water flow through the bioreactors was delayed by at least 24 hours, beginning late in the day on May 22 and ending on May 26 (Figure 23). The impact of the rain event was observed as a sharp decrease in depth to groundwater during recharge (Figure 10). On May 23, after two days of rainfall, dissolved nitrate-N in groundwater was 18 ppm at 1.2 m and 1 ppm at 2 m. On May 28, groundwater was again observed to increase in concentration

towards the soil surface, with readings of 28 ppm, 17 ppm, and 2 ppm NO_3^--N at 60 cm, 120 cm, and 200 cm depths respectively (Figure 22), indicating N leaching from the soil surface and attenuation with depth. A portion of the leached N was captured by drainage tile laterals located ~1 m below the soil surface and directed towards the pre-bioreactor control structures ("BBR").

5.2.2 Bioreactor Performance

Elevated levels of NO_3^--N, but not NO_2^--N or NH_4^+-N were present in the tile water (Figure 31). Tile water was held by stop-gates set at 0.59 m from the base of the control structures, and was unable to flow into the bioreactors until sufficient water accumulated to overflow the stop-gate. The delay between the start of the rain event and the beginning of the tile flow event was due to rainwater infiltration time through the silt loam soil, as well as restriction by the controlled tile drainage system. This delay allowed rainwater to accumulate inside the reactor beds for at least 24 hours prior to the commencement of tile water flow. The majority of the 66 mm of rainfall occurred prior to tile flow (Figure 9). Once water began flowing through the BBR control structure (see Figure 4), it was able to travel through either the bioreactor or through the bypass. The stop-gate configurations were set such that the majority of flow would bypass the bioreactors. This aggressive bypass ratio was intended to assess the reactor substrate, and while not typical, the impact of increasing the proportion of bypass flow is an increase in residence time which should improve N removal performance.

The $\delta^{15}N$ signature of NO_3 in tile water entering the bioreactors ranged from +11‰ to +15‰, and was more enriched than total N of manure (Figure 14), soil (Figure 19 and Figure 20), and corn plants (Figure 15 and Figure 16). The fact that nitrate ^{15}N was more enriched than manure N

and soil N indicates that nitrate was enriched by denitrification in soil, since conversion of organic N or ammonium N to nitrate generates relatively ^{15}N-depleted nitrate (see Section 1.5).

Denitrification of nitrate is stimulated in denitrifying bioreactors by increasing the availability of carbon. Bioreactor N-removal performance is sensitive to factors such as residence time, temperature, source of carbon, and nutrient loading rate (Liang et al., 2015; Warneke et al., 2011b), but in general, denitrifying bioreactors have been shown to successfully remove agricultural nitrate from tile water (Warneke et al., 2011a). Controlled tile drainage has been shown to increase residence time when paired with bioreactors, leading to greater N removal (Woli et al., 2010). Complete denitrification to N_2 does not always occur however, and a portion of NO_3^--N is emitted as N_2O. Khalil et al. (2004) found that the ratio of N_2O:N_2 gas production by denitrifiers was between 6% and 13%, in treatments where the partial pressure of O_2 was held at 0 and 0.35 kPa. This ratio was found to increase substantially with O_2 >0.35 kPa where nitrification plays a more significant role; however, anaerobic denitrification had a much higher emission rate and resulted in the largest production of N_2O. Dissolved oxygen levels of above 0.5 mg L^{-1} have been shown to not limit NO_3^--N removal in a reactor bed (Warneke et al., 2011b).

N_2O produced in denitrifying bioreactors can be lost by upward diffusion to the soil surface, or carried through tile water effluent as dissolved N_2O. Woli et al. (2010) reported N_2O surface emissions of 10.2 to 130.2 µg N m^{-2} h^{-1} from beds treating drainage water. Ghane et al. (2015) found N_2O surface emissions above active bioreactors were only 0.6 to 17.4 µg N m^{-2} h^{-1}, and equated to 0.002% of N inputs on average. As a result, it was recommended that future studies evaluate the export dissolved N_2O as well. Elgood et al. (2010) observed denitrifying bioreactors in southern Ontario that produced dissolved N_2O at up to 100 µg N m^{-2} h^{-1}, occurring mainly in

the winter and spring months and accounting for at most 2% of NO_3^- removal, whereas in the hottest summer months the reactors acted as an N_2O sink. Warneke et al. (2011b) observed nitrate removal in a large denitrification bed with high NO_3^- concentration (>100 g N m^{-3}) and found that 1% of the removed NO_3^-N was released as N_2O from the bed surface (4715 µg N m^{-2} h^{-1}), while a further 3.3% was released as dissolved N_2O (15 g N_2O-N h^{-1}).

In this study, a decrease in both NO_3^--N and dissolved N_2O-N was observed through the bioreactors (Figure 32 and Figure 33). An average decrease in dissolved N_2O of 60 ±22% was observed, and the percent decrease in dissolved N_2O at each of the reactors was strongly correlated (+0.80) with the percent decrease in nitrate (Figure 34), suggesting that the same process acted on both N species equally. If denitrification were responsible for the decrease in nitrate-N through the bioreactors, we would expect to see N_2O produced and emitted from the system either at the soil surface, or as dissolved N_2O in reactor effluent.

Soil gas flux above all bioreactors was sampled regularly throughout 2012 (Figure 12) and 2013 (Figure 13), and coincided with tile water flow events through bioreactors on six dates during the 2013 season (June 3, June 7, September 24, November 7, November 14, November 21). Typical soil flux observed during these events were <10 µg m^{-2} h^{-1}. The reactor beds were covered only by a permeable geotextile fabric and ~0.5 m of overlying soil; therefore, chambers placed directly above reactor beds were able to capture emissions. In-field chamber measurements successfully captured N_2O fluxes of over 800 µg m^{-2} h^{-1} in spring 2013 in the Winchester fields (Figure 13), however emissions over reactor beds ranged from minor to undetectable. Although gas sampling did not always coincide with tile water flow through bioreactors, denitrification continues without water flow since residual tile water remains inside the bioreactors.

An approximation of the expected soil gas flux above reactor beds was calculated given the observed decrease in nitrate through the reactors, for several theoretical N_2O:N_2 gas production ratios between 1% and 20% (Table 6). The expected fluxes were significantly higher than any observed over bioreactors in 2012 or 2013 when calculated using a modest 5% N_2O:N_2 emission ratio, and higher than the largest observed flux at any reactor throughout the 2013 growing season (57 $\mu g\ m^{-2}\ h^{-1}$).

The strongest indicator of denitrification is the comparison of $\delta^{15}N$ signature of NO_3^- before and after bioreactor treatment. Denitrification of NO_3^- to N_2 follows a Rayleigh distillation with a net $\delta^{15}N$ enrichment factor of +20‰ to +30‰ (Section 1.5). Using the known concentrations of nitrate before and after bioreactor treatment and a modest +20 ‰ enrichment factor, Equation 4 predicts a much higher $\delta^{15}N$-NO_3^- compared with what was observed from the reactors (Figure 38). The disparity between observed versus expected isotopic enrichment is direct evidence demonstrating a lack of kinetic fractionation that is characteristic of denitrification. This is particularly notable given the extended residence time provided by an aggressive bypass ratio during this period. The fact that this did not occur indicates that denitrification was not the primary means of N loss, and therefore one or more alternatives must be investigated.

Anaerobic ammonium oxidation (Anammox) is an N transformation pathway found in oxygen poor environments and involves simultaneous oxidation of ammonium and reduction of nitrate to produce N_2 (Mulder et al., 1995). The required nitrite may be seeded by aerobic ammonium oxidation, in which case nitrate would not be consumed, or by partial denitrification of NO_3^- which would produce isotope effects in ^{15}N-NO_3 which were not observed (Figure 38). Ammonium-N concentrations in tile water were consistently below 5 ppm throughout the Spring;

therefore, there was insufficient ammonium to facilitate anammox reactions of the scale required to remove up to 17 ppm of NO_3^-N, and the reaction would have been limited by ammonium availability. Additionally, the observed decrease in dissolved N_2O cannot be attributed to anammox as N_2O is not involved in anammox reactions.

A second alternative considered was simultaneous nitrification of NH_4^+ to NO_3^-, and denitrification of NO_3^- to N_2, such that the final $\delta^{15}N$ signature of NO_3^- remained the same. It is possible that highly ^{15}N-depleted nitrate was added to the nitrate pool in sufficient proportion to offset the enrichment by denitrifiers. This could have resulted in a $\delta^{15}N$-NO_3 signature mirroring the original ^{15}N enrichment while allowing for an overall decrease in nitrate concentration, but is deemed extremely unlikely since all six bioreactors would have had to experience this combination of reactions while maintaining $\delta^{15}N$-NO_3^- within a narrow range. Furthermore, no known source of highly ^{15}N-depleted ammonium was present, ammonium in tile water was found to be below 5 ppm N throughout the spring (Figure 31).

The final alternative to denitrification examined was dilution of tile water within the reactor beds. Mixing of the nitrate-rich tile water with one or more sources of N-poor or fresh water would account for the decline in post-bioreactor nitrate and dissolved nitrous oxide, while also exhibiting no isotope effects (see Figure 2). At reactor T3, a decrease in nitrate was observed after treatment on May 23 (Figure 27) but not on May 24 (Figure 32). This reactor also had the highest water flow rate. If the mixing occurring inside the bioreactors was between a fixed quantity of pre-existing water and incoming tile water, the tile water would eventually displace all of the existing water and dilution would eventually cease. This would occur first at the reactor with the the greatest cumulative water flow. A strong negative correlation (-0.8) was observed

between the percent decrease of nitrate and average flowrate of tile water passing through the reactors at the time of sampling (Figure 35). Dilution also provides an explanation for the lack of N_2O flux observed above bioreactors since it is a non-transformative process.

Two possible methods of dilution include mixing of groundwater and infiltration of rainwater. Infiltration by groundwater was limited by an impermeable plastic lining along the base and walls of each reactor bed; however, it is theoretically possible that some infiltration occurred along seams. The water table was observed at approximately 1 m below surface prior to, and between 30-80 cm below surface during the rain event (Figure 10). Based on the dimensions of the reactor beds, the water table was above the bottom of the reactor beds between mid-March and mid-July 2013 enabling the possibility for groundwater penetration. The bioreactors were designed to be impermeable, and were underlain by clay soil with a vertical $K_{sat} = 10^{-7}$ cm s^{-1}, making this hypothesis unlikely, especially since impacts were observed in multiple reactors.

Infiltration of rain water has the potential to contribute fresh water directly to the reactor via the permeable fabric cover over the woodchip beds. Rainfall began on May 21 (Figure 9), and due to the use of a controlled tile drainage system, tile water was prevented from entering the reactors until May 23 (Figure 23), allowing 1-2 days of rainfall to accumulate inside the bioreactors. The nearest climate station measured approximately 60 mm of rainfall over a 72-hr period between May 21 and 23. Multiplying by the area of the bioreactors (3.73 m^2) gives ~220 L of rainwater potentially added to each 3.7 m^2 bioreactor. In addition to the contribution of rainwater from May 21-23, water from prior rain events, tile flow events, and/or spring snowmelt may have been present in the reactors, and retained by the control structures located upstream and downstream.

6. Conclusions and Future Work

Manure N was demonstrated to have been leached from the soil surface where it was partially denitrified. Significant soil N_2O emissions occurred at several times throughout the field seasons, usually following the application of manure or precipitation events, indicating the presence of denitrification. Leached nitrate from soil was observed to be captured in drainage tiles and a portion passed through the bioreactors.

Denitrifying bioreactors have been shown to be an effective technology for removing nitrate from agricultural tile effluent. Previous studies have demonstrated that denitrification of nitrate in bioreactors elicits the production of N_2O, which is emitted from the overlying soil surface and/or is released as dissolved N_2O in tile effluent. In comparison, this study demonstrated a situation in which a decrease in nitrate was associated with decreasing levels of nitrous oxide, and no significant N_2O flux was recorded above bioreactors throughout the year. The $\delta^{15}N$ and $\delta^{18}N$ signatures of nitrate also did not change significantly following bioreactor treatment and did not exhibit the ^{15}N and ^{18}O enrichment that is characteristic of denitrification. The data demonstrate that the decrease in nitrate through the bioreactors was due to dilution, likely from the accumulation of rainfall in reactor beds employing controlled tile drainage. As a result, the hypothesis that the treatment of nitrate in the bioreactors would generate N_2O was disproved, and the hypothesis that the $\delta^{15}N$ and $\delta^{18}O$ signatures of residual nitrate would increase following bioreactor treatment was disproved.

Future investigative work is recommended to identify the water flow paths surrounding the bioreactors during tile water flow events, and to pinpoint the conditions under which dilution may occur. Installation of a rain gauge on site and water loggers in reactor beds is recommended

to understand how water accumulates in the reactors, and how water level fluctuates with precipitation and snowmelt. The lack of significant N_2O flux above bioreactors in measurements taken throughout 2012 and 2013 does not necessarily indicate lack of denitrification, but suggests that the majority of N_2O produced by denitrification may be exiting the reactor beds as dissolved N_2O. Future work should include the regular monitoring of $\delta^{15}N$ of nitrate and dissolved nitrous oxide, and concentration of dissolved oxygen, to demonstrate correct functioning of the bioreactors and to determine when and why denitrification may not occur. A nitrogen mass balance of the bioreactors during a similar tile flow event, including the measurement of N_2:Ar, is suggested to identify and quantify denitrification.

7. References

Agriculture and Agri-Food Canada, 2000. Agricultural Best Management Practices, Water Quality Matters.

Aulakh, M.S., Doran, J.W., Mosier, A.R., 1992. Soil Denitrification—Significance, Measurement, and Effects of Management, in: Stewart, B.A. (Ed.), Advances in Soil Science. Springer New York, New York, NY, pp. 1-57.

Barford, C.C., Montoya, J.P., Altabet, M.A., Mitchell, R., 1999. Steady-state nitrogen isotope effects of N2 and N2O production in Paracoccus denitrificans. Applied and Environmental Microbiology 65, 989-994.

Beauchamp, E.G., 1986. AVAILABILITY OF NITROGEN FROM THREE MANURES TO CORN IN THE FIELD. Canadian Journal of Soil Science 66, 713-720.

Bernhard, A., 2010. The Nitrogen Cycle: Processes, Players, and Human Impact. Nature Education Knowledge 3.

Bock, E., Smith, N., Rogers, M., Coleman, B., Reiter, M., Benham, B., Easton, Z.M., 2015. Enhanced nitrate and phosphate removal in a denitrifying bioreactor with biochar. Journal of environmental quality 44, 605-613.

Bouwman, L., Goldewijk, K.K., Van Der Hoek, K.W., Beusen, A.H.W., Van Vuuren, D.P., Willems, J., Rufino, M.C., Stehfest, E., 2013. Exploring global changes in nitrogen and phosphorus cycles in agriculture induced by livestock production over the 1900-2050 period. Proceedings of the National Academy of Sciences of the United States of America 110, 20882-20887.

Brand, W.A., 1995. PreCon: A Fully Automated Interface for the Pre-Gc Concentration of Trace Gases on Air for Isotopic Analysis. Isotopes in environmental and health studies 31, 277-284.

Bundy, L.G., 1998. Corn Fertilization, Cooperative Extension. University of Winsconsin.

Burns, L.C., Stevens, R.J., Laughlin, R.J., 1995. Determination of the simultaneous production and consumption of soil nitrite using 15N. Soil Biology and Biochemistry 27, 839-844.

Butterbach-Bahl, K., Baggs, E.M., Dannenmann, M., Kiese, R., Zechmeister-Boltenstern, S., 2013. Nitrous oxide emissions from soils: how well do we understand the processes and their controls? Philosophical transactions of the Royal Society of London. Series B, Biological sciences 368, 20130122.

Casciotti, K.L., 2009. Inverse kinetic isotope fractionation during bacterial nitrite oxidation. Geochimica et Cosmochimica Acta 73, 2061-2076.

Casciotti, K.L., Sigman, D.M., Ward, B.B., 2003. Linking diversity and stable isotope fractionation in ammonia-oxidizing bacteria. Geomicrobiology Journal 20, 335-353.

Christianson, L.E., Bhandari, A., Helmers, M.J., 2011a. Pilot-Scale Evaluation of Denitrification Drainage Bioreactors: Reactor Geometry and Performance. Journal of Environmental Engineering 137, 213-220.

Christianson, L.E., Hanly, J.A., Hedley, M.J., 2011b. Optimized denitrification bioreactor treatment through simulated drainage containment. Agricultural Water Management 99, 85-92.

Clark, I., 2015. Groundwater Geochemistry and Isotopes. CRC Press.

Clark, I.F., Peter, 1997. Environmental Isotopes in Hydrogeology. CRC Press LLC.

Coyotzi, S.P., P; Clark, I.D.; Lapen, D.R.; Van Cappellen, P; Doxey, A.C.; Neufeld, J.D., 2016. Active agricultural soil denitrifiers possess extensive nitrite reductase gene diversity. Environ. Microbiol. Submitted.

Crabbé, P., Lapen, D.R., Clark, H., Sunohara, M., Liu, Y., 2012. Economic benefits of controlled tile drainage: Watershed Evaluation of Beneficial Management Practices, South Nation River basin, Ontario. Water Quality Research Journal of Canada 47, 30-41.

De Freitas, J.R., Schoenau, J.J., Boyetchko, S.M., Cyrenne, S.A., 2003. Soil microbial populations, community composition, and activity as affected by repeated applications of hog and cattle manure in eastern Saskatchewan. Can J Microbiol 49, 538-548.

del Prado, A., Merino, P., Estavillo, J.M., Pinto, M., González-Murua, C., 2006. N2O and NO emissions from different N sources and under a range of soil water contents. Nutrient Cycling in Agroecosystems 74, 229-243.

Delwiche, C.C., Steyn, P.L., 1970. Nitrogen isotope fractionation in soils and microbial reactions. Environmental Science & Technology 4, 929-935.

Duarte, C.M., 2009. Coastal eutrophication research: a new awareness. Hydrobiologia 629, 263-269.

Elgood, Z., Robertson, W.D., Schiff, S.L., Elgood, R., 2010. Nitrate removal and greenhouse gas production in a stream-bed denitrifying bioreactor. Ecological Engineering 36, 1575-1580.

Environment Canada, 2013. Canada's Emissions Trends.

Environment Canada, 2015a. Canadian Climate Normals 1981-2010 Station Data for Kemptville, Ontario.

Environment Canada, 2015b. National Inventory Report 1990-2013.

EPA, U.S., 2002. Nitrification.

Erisman, J.W., Sutton, M.A., Galloway, J., Klimont, Z., Winiwarter, W., 2008. How a century of ammonia synthesis changed the world. Nature Geoscience 1, 636-639.

Fields, S., 2004. Global Nitrogen: Cycling out of Control. Environmental Health Perspectives 112, A556-A563.

Fowler, D., Steadman, C.E., Stevenson, D., Coyle, M., Rees, R.M., Skiba, U.M., Sutton, M.A., Cape, J.N., Dore, A.J., Vieno, M., Simpson, D., Zaehle, S., Stocker, B.D., Rinaldi, M., Facchini, M.C., Flechard, C.R., Nemitz, E., Twigg, M., Erisman, J.W., Butterbach-Bahl, K., Galloway, J.N., 2015. Effects of global change during the 21st century onthe nitrogen cycle. Atmospheric Chemistry and Physics 15, 13849-13893.

Fraser, H.F., Ron, 2001. Environmental Benefits of Tile Drainage - Literature Review. University of Guelph.

Galloway, J.N., 1998. The global nitrogen cycle: Changes and consequences. Environmental Pollution 102, 15-24.

Galloway, J.N., Aber, J.D., Erisman, J.W., Seitzinger, S.P., Howarth, R.W., Cowling, E.B., Cosby, B.J., 2003. The Nitrogen Cascade. BioScience 53, 341-356.

Ghane, E., Fausey, N.R., Brown, L.C., 2015. Modeling nitrate removal in a denitrification bed. Water research 71, 294-305.

Graham, P.H., Vance, C.P., 2003. Legumes: Importance and constraints to greater use. Plant Physiology 131, 872-877.

Granger, J., Sigman, D.M., Prokopenko, M.G., Lehmann, M.F., Tortell, P.D., 2006. A method for nitrite removal in nitrate N and O isotope analyses. Limnology and Oceanography: Methods 4, 206-212.

Hernandez-Ramirez, G., Brouder, S.M., Smith, D.R., Van Scoyoc, G.E., 2009. Greenhouse gas fluxes in an eastern corn belt soil: Weather, nitrogen source, and rotation. Journal of environmental quality 38, 841-854.

Huijsmans, J., 2003. Effect of application method, manure characteristics, weather and field conditions on ammonia volatilization from manure applied to arable land. Atmospheric Environment 37, 3669-3680.

Hutchinson, G.L., Livingston, G.P., 2001. Vents and seals in non-steady-state chambers used for measuring gas exchange between soil and the atmosphere. European Journal of Soil Science 52, 675-682.

IPCC, 2007a. Climate Change 2007: Working Group I: The Physical Science Basis, IPCC Fourth Assessment Report: Climate Change 2007.

IPCC, 2007b. Climate Change 2007: Working Group I: The Physical Science Basis, IPCC Fourth Assessment Report: Climate Change 2007.

Kendall, C., Aravena, R., 2000. Nitrate Isotopes in Groundwater Systems, in: Cook, P.G., Herczeg, A.L. (Eds.), Environmental Tracers in Subsurface Hydrology. Springer US, Boston, MA, pp. 261-297.

Khalil, K., Mary, B., Renault, P., 2004. Nitrous oxide production by nitrification and denitrification in soil aggregates as affected by O2 concentration. Soil Biology and Biochemistry 36, 687-699.

Lapen, D.R., Topp, E., Edwards, M., Sabourin, L., Curnoe, W., Gottschall, N., Bolton, P., Rahman, S., Ball-Coelho, B., Payne, M., Kleywegt, S., McLaughlin, N., 2008. Effect of liquid municipal biosolid application method on tile and ground water quality. Journal of environmental quality 37, 925-936.

Lepori, F., Keck, F., 2012. Effects of atmospheric nitrogen deposition on remote freshwater ecosystems. Ambio 41, 235-246.

Létolle, R., 1980. Nitrogen-15 in the natural environment., in: Fritz, P.F., J.Ch. (Ed.), Handbook of Environmental Isotope Geochemistry, Volume 1: The Terrestrial Environment. Elsevier.

Liang, X., Lin, L., Ye, Y., Gu, J., Wang, Z., Xu, L., Jin, Y., Ru, Q., Tian, G., 2015. Nutrient removal efficiency in a rice-straw denitrifying bioreactor. Bioresour Technol 198, 746-754.

Maag, M., Vinther, F.P., 1996. Nitrous oxide emission by nitrification and denitrification in different soil types and at different soil moisture contents and temperatures. Applied Soil Ecology 4, 5-14.

Mariotti, A., Germon, J.C., Hubert, P., Kaiser, P., Letolle, R., Tardieux, A., Tardieux, P., 1981. Experimental determination of nitrogen kinetic isotope fractionation: Some principles; illustration for the denitrification and nitrification processes. Plant and Soil 62, 413-430.

Matthews, B.C.R., N.R., 1952. Soil Survey of Dundas County, Ontario Soil Survey. Canada Department of Agriculture and the Ontario Agriculture College, Guelph, Ontario.

Meade, G., Pierce, K., O'Doherty, J.V., Mueller, C., Lanigan, G., Mc Cabe, T., 2011. Ammonia and nitrous oxide emissions following land application of high and low nitrogen pig manures to winter wheat at three growth stages. Agriculture, Ecosystems & Environment 140, 208-217.

Michalski, G., Kolanowski, M., Riha, K.M., 2015. Oxygen and nitrogen isotopic composition of nitrate in commercial fertilizers, nitric acid, and reagent salts. Isotopes in environmental and health studies 51, 382-391.

Millar, N., Robertson, G.P., Grace, P.R., Gehl, R.J., Hoben, J.P., 2010. Nitrogen fertilizer management for nitrous oxide (N2O) mitigation in intensive corn (Maize) production: an emissions reduction protocol for US Midwest agriculture. Mitigation and Adaptation Strategies for Global Change 15, 185-204.

Moorman, T.B., Parkin, T.B., Kaspar, T.C., Jaynes, D.B., 2010. Denitrification activity, wood loss, and N2O emissions over 9 years from a wood chip bioreactor. Ecological Engineering 36, 1567-1574.

Mulder, A., van de Graaf, A.A., Robertson, L.A., Kuenen, J.G., 1995. Anaerobic ammonium oxidation discovered in a denitrifying fluidized bed reactor. FEMS Microbiology Ecology 16, 177-183.

OMAFRA, 2009. Soil Fertility and Nutrient Use: Manure Management.

OMAFRA, 2016. Best Management Practices Series.

Ostrom, N.E., Pitt, A., Sutka, R., Ostrom, P.H., Grandy, A.S., Huizinga, K.M., Robertson, G.P., 2007. Isotopologue effects during N2O reduction in soils and in pure cultures of denitrifiers. Journal of Geophysical Research: Biogeosciences 112, n/a-n/a.

Rochette, P., Bertrand, N., 2003. Soil air sample storage and handling using polypropylene syringes and glass vials. Canadian Journal Soil Science 83, 631-637.

Rochette, P., Bertrand, N., 2008. Soil-Surface Gas Emissions, in: Carter, M.R., Gregorich, E.G. (Eds.), Soil Sampling and Methods of Analysis, 2nd ed. CRC Press Taylor & Francis.

Rozemeijer, J.C., Visser, A., Borren, W., Winegram, M., Van Der Velde, Y., Klein, J., Broers, H.P., 2016. High-frequency monitoring of water fluxes and nutrient loads to assess the effects of controlled drainage on water storage and nutrient transport. Hydrology and Earth System Sciences 20, 347-358.

Shearer, G.K., D.H., 1989. Estimates of N2 Fixation in Ecosystems: The Need for and Basis of the 15N Natural Abundance Method, in: Rundel, P.E., J.R.; Nagy, K.A. (Ed.), Stable Isotopes in Ecological Research. Springer-Verlag, p. 347.

Smil, V., 2002a. Nitrogen and Food Production: Proteins for Human Diets. AMBIO: A Journal of the Human Environment 31, 126-131.

Smil, V., 2002b. Nitrogen and food production: Proteins for human diets. Ambio 31, 126-131.

Statistics Canada, 2015. Fertilizer Shipments Survey.

Sunohara, M.D., Craiovan, E., Topp, E., Gottschall, N., Drury, C.F., Lapen, D.R., 2014. Comprehensive nitrogen budgets for controlled tile drainage fields in eastern ontario, Canada. Journal of environmental quality 43, 617-630.

Verhallen, A.L., Janice, 2004. Understanding Nitrogen. Ontario Ministry of Agriculture, Food and Rural Affairs.

Warneke, S., Schipper, L.A., Bruesewitz, D.A., Baisden, W.T., 2011a. A comparison of different approaches for measuring denitrification rates in a nitrate removing bioreactor. Water research 45, 4141-4151.

Warneke, S., Schipper, L.A., Bruesewitz, D.A., McDonald, I., Cameron, S., 2011b. Rates, controls and potential adverse effects of nitrate removal in a denitrification bed. Ecological Engineering 37, 511-522.

Warneke, S., Schipper, L.A., Matiasek, M.G., Scow, K.M., Cameron, S., Bruesewitz, D.A., McDonald, I.R., 2011c. Nitrate removal, communities of denitrifiers and adverse effects in different carbon substrates for use in denitrification beds. Water research 45, 5463-5475.

Weiss, R.F., Price, B.A., 1980. Nitrous oxide solubility in water and seawater. Mar. Chem. 8, 347-359.

Woli, K.P., David, M.B., Cooke, R.A., McIsaac, G.F., Mitchell, C.A., 2010. Nitrogen balance in and export from agricultural fields associated with controlled drainage systems and denitrifying bioreactors. Ecological Engineering 36, 1558-1566.

Yoshida, N., 1988. 15N-depleted N2O as a product of nitrification. Nature 335, 528-529.

Zingore, S., Delve, R.J., Nyamangara, J., Giller, K.E., 2007. Multiple benefits of manure: The key to maintenance of soil fertility and restoration of depleted sandy soils on African smallholder farms. Nutrient Cycling in Agroecosystems 80, 267-282.